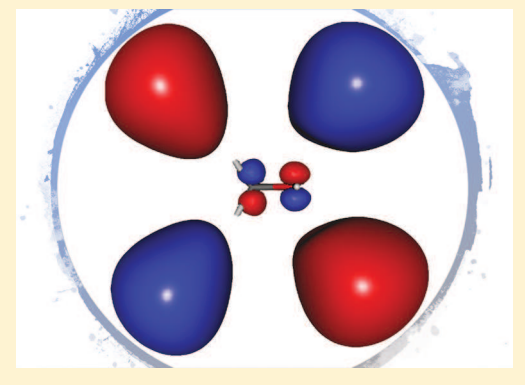
Electronic Structure of Liquid Methanol and Ethanol from Polarization-Dependent Two-Photon Absorption Spectroscopy

Published as part of The Journal of Physical Chemistry virtual special issue "Hanna Reisler Festschrift". Dhritiman Bhattacharyya, Yuyuan Zhang, Christopher G. Elles, and Stephen E. Bradforth

Department of Chemistry, University of Southern California, Los Angeles, California 90089-0482, United States

Supporting Information

ABSTRACT: Two-photon absorption (2PA) spectra of liquid methanol and ethanol are reported for the energy range 7-10 eV from the first electronic excitation to close to the liquid-phase ionization potential. The spectra give detailed information on the electronic structures of these alcohols in the bulk liquid. The focus of this Article is to examine the electronic structure change compared with water on substitution of a hydrogen by an alkyl group. Continuous 2PA spectra are recorded in the broadband pump-probe fashion, with a fixed pump pulse in the UV region and a white-light continuum as a probe. Pump pulses of two different energies, 4.6 and 6.2 eV, are used to cover the spectral range up to 10 eV. In addition, theoretical 2PA cross sections for both molecules isolated in the gas phase are computed by the equation-of-motion coupled-cluster method with single and double substitutions (EOM-CCSD). These computational



results are used to assign both the experimental 2PA and literature one-photon linear absorption spectra. The most intense spectral features are due to transitions to the Rydberg states, and the 2PA spectra are dominated by the totally symmetric $3p_z \leftarrow$ 2pz transition in both alcohols. The experimental 2PA spectra are compared with the simulated 2PA spectra based on ab initio calculations that reveal a general blue shift of the excited transitions upon solvation. The effective 2PA thresholds in methanol and ethanol decrease to 6.9 eV compared with 7.8 eV for water. The analysis of the 2PA polarization ratio leads us to conclude that the excited states of ethanol deviate more markedly from water in the lower energy region compared with methanol. The polarization dependence of the 2PA spectra reveal the symmetries of the excited states within the measured energy range. Natural transition orbital calculations are performed to visualize the nature of the transitions and the orbitals participating during electronic excitation.

I. INTRODUCTION

One-photon (1PA) and two-photon absorption (2PA) spectroscopies are two complementary techniques because they are governed by different selection rules. Information from both techniques together can help provide a complete picture of the electronic excited states of a molecule or material. Moreover, the polarization dependence of 2PA spectroscopy gives information about the symmetry of the electronic excited states. 2PA has been widely used in many condensed-phase applications; 1-13 however, the 2PA cross sections (σ_{2PA}) of common solvents, which are typically obtained at a single wavelength via the traditional z-scan technique, are sparse in the literature. ^{14–21} In comparison, broadband spectra analogous (and complementary) to conventional linear UV-visible 1PA spectra are available for only a handful of much larger systems such as retinal, ²² C₆₀, ²³ porphyrins, ^{24–27} ZnS nanocrystals, ^{28,29} stilbene and phenanthrene, ^{30–32} and hydroxyphenacyl phototriggers. ³³ Previously, we reported the broadband 2PA spectrum of water in the 7-10 eV range.³⁴ In this Article, we have extended our study to the prototypical alcohols: methanol and ethanol. The main

focus will be to analyze the nature of the electronic excited states and how the 2PA spectrum changes due to the substitution of one of the hydrogens in water by an alkyl group.

The 2PA cross sections of common solvents have been reported by several groups at discrete energies; 16-18 however, a comprehensive understanding of the excited states or even the determination of the 2PA band gap is next to impossible with such a few data points. Liquid jet photoelectron spectroscopy experiments on methanol show that the vertical ionization energy (VIE) decreases from 10.94 to 9.99 eV on going from the gas to the liquid phase.³⁵ Despite this, liquid methanol can be adiabatically ionized down to its optical absorption edge at \sim 4.7 eV, which is \sim 5.3 eV less than the VIE. ³⁶ A similar phenomenon is true for liquid water.^{37–39} Explaining such phenomena demands a better visualization of electronic structure and understanding the fate of the optically bright Rydberg states in the condensed phase. There is abundant

Received: April 30, 2019 Revised: June 12, 2019 Published: June 14, 2019



The Journal of Physical Chemistry A

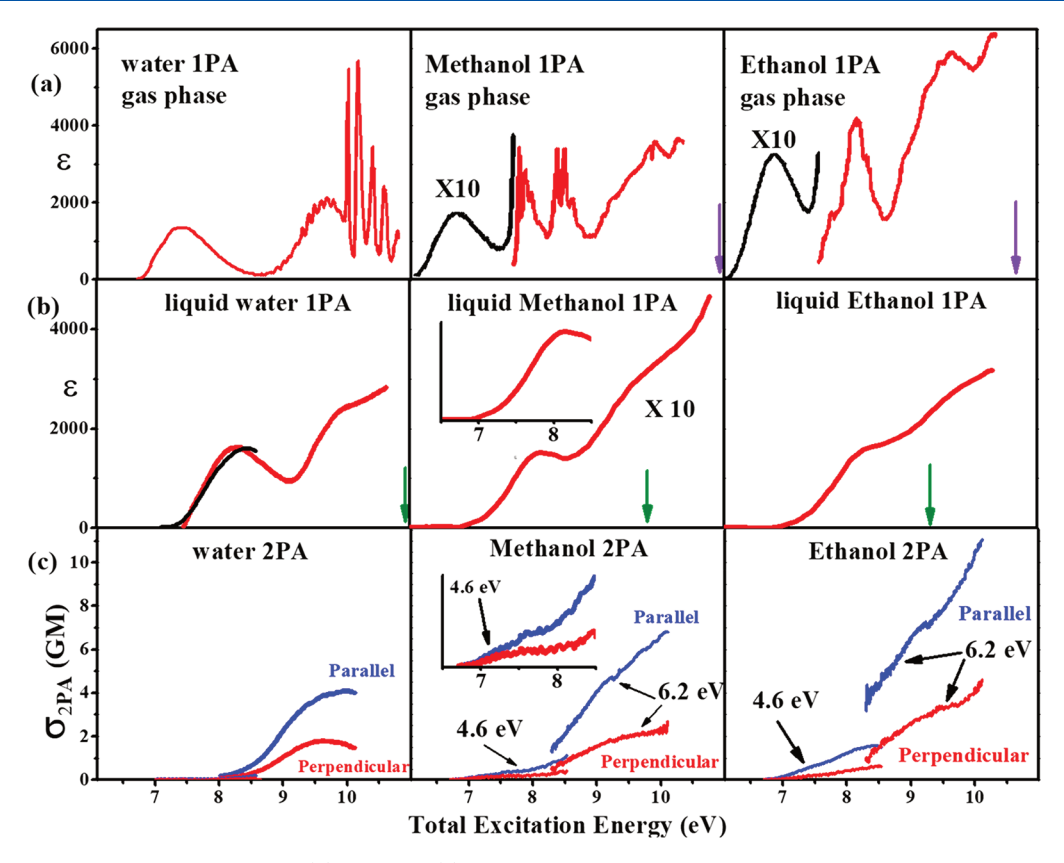


Figure 1. (a) Gas-phase 1PA and liquid-phase (b) 1PA and (c) 2PA spectra of water, methanol, and ethanol. The water gas-phase spectrum is digitized from ref 57 and is converted to ε (L mol⁻¹ cm⁻¹) using the equation $\varepsilon = (N_A/\ln(10))\sigma_{1PA}$, where σ_{1PA} and N_A are the 1PA cross section and the Avogadro constant, respectively. The alcohol gas-phase spectra are digitized from ref 58 and converted to ε using the $A = \varepsilon cl$ equation, where the path length l is 1 μ m. The water liquid-phase 1PA spectrum is from refs 59 and 60, and the 1PA spectra of liquid alcohols are from ref 61. (c) 2PA spectra for water, methanol, and ethanol. The water 2PA spectrum is from ref 34. The data for the alcohols are from this work. Spectra recorded with both a 4.6 and a 6.2 eV pump are shown in the same panel. Parallel (blue) and perpendicular polarization (red). The purple and green arrows show the positions of the vertical ionization energies in the gas phase 35 and the liquid phase, 62 respectively. The VIE of water vapor is 12.62 eV 35 and is outside the spectral range shown in the above plot. (Insets) For liquid MeOH, 1PA and 2PA showing detail from 6.5 to 8.5 eV.

literature 40-44 concentrating on the interaction of a Rydberg state with other Rydberg or valence states in isolated molecular systems. Describing such interactions has emerged as a challenging problem in electronic structure theory. Failing to accurately quantify the coupling between these states can dramatically affect the calculated electronic properties, such as the transition dipole and the shape of the potential energy surfaces. 45,46 Regarding Rydberg states in condensed environments, pioneering work has been carried out by Chergui and coworkers, who investigate the fate of Rydberg orbitals in condensed media by trapping the NO molecule in both molecular matrices ^{47,48} and rare gas matrices. ^{49,50} Optical excitation to a Rydberg state leads to an increase in the spatial distribution of the electrons, giving rise to a large change in the molecule-matrix interaction. The gas-to-matrix shift of absorption energies and the broadening of absorption bands are functions of the size of the matrix cage and the nature of the excited Rydberg orbital (s, p, or d type).⁵¹ In the case of NO, lengthening of the fluorescence lifetime of a molecular Rydberg state when going from isolation to condensed media⁵² points to the fact that the local structure of the solvent environment has considerable influence on the transition dipole. Furthermore, because of mixing of Rydberg orbitals with the solvent continuum, the characterization of these orbitals below the VIE provides invaluable information on the competing ionization and dissociation channels. 36,53,54 Al-

brecht and coworkers considered liquid benzene and benzene diluted in hexane via two-photon excitation spectra. ^{55,56} This study pointed out that the dominance of a Rydberg excitation between 6 and 7 eV, which was well known in the gas phase, also played an important role in the liquid solution. The favorable selection rules for two-photon excitation were important in uncovering this state.

To get a better picture of the Rydberg contribution to the electronic structure of other important bulk molecular liquid solvents, the simple sigma-bonded liquids methanol and ethanol are amenable to analysis because of the lack of lowlying valence excitations. Here we report on the continuous 2PA spectra of these liquid alcohols in the energy range 6.8-10.2 eV. Two different pump energies (4.6 and 6.2 eV) have been used to cover the region of the spectra. By changing the relative polarization of pump and probe photons, both parallel and perpendicularly polarized spectra have been reported, along with the polarization ratio (ρ) , which is defined as (σ_{para}) $\sigma_{
m perp}$), where $\sigma_{
m para}$ and $\sigma_{
m perp}$ are parallel and perpendicular 2PA cross sections, respectively. Theoretical 2PA cross sections for transitions from ground to several excited states are calculated for isolated methanol and ethanol molecules, and they provide a useful starting point in assigning the nature of the transitions that have significant contribution toward the 2PA spectra.

II. BACKGROUND: 1PA SPECTRUM OF METHANOL AND ETHANOL

The gas-phase spectrum of alcohols is a very good starting point for identifying excited electronic states before we delve into the more complicated liquid system. The gas-phase 1PA spectra of methanol and ethanol, 58 shown in Figure 1a, reveal the lowest energy band at ~6.7 eV. This band is very weak in intensity and is due to the 3s \leftarrow 2p_z orbital promotion on oxygen (z axis is defined as out-of-plane), as pointed out by Cheng et al.⁵³ The broadness of this band comes from the dissociative nature of the potential energy surface of the 1A" upper state; although the 1A" state is predominantly Rydberg in nature, it acquires antibonding character along the O-H vibrational coordinate due to interaction with states of the same symmetry. 53,63 The oscillator strength of the similar character transition is almost 10 times stronger in the case of water. A similar result is obtained in our ab initio calculation (vide infra), where the oscillator strength of this transition is seen to be reduced from 0.05 in water to 0.004 in methanol. This reduction is the consequence of the delocalization of the 3s Rydberg orbital of oxygen over the alkyl groups of the alcohols, which makes the transition moment integral $\langle n_0 | e \cdot r |$ 3s) decrease with the increasing size of the alkyl group. 63 The first gas-phase 1PA band $(3s \leftarrow 2p_z)$ is red-shifted by 0.7 eV as compared with water. The alkyl group, being electron donating in nature, can be considered to push the electron density toward the oxygen atom, which results in increasing electronelectron repulsion and thereby destabilizes the lone pairs on oxygen (HOMO and HOMO-1). This is consistent with the drop of first vertical ionization potential from water to methanol to ethanol.64,65

As can be seen in Figure 1a, in MeOH, the two clusters of sharp bands in the region of 7.7 to 9.0 eV are transitions from HOMO (2p_z) to the 3p Rydberg orbitals. ^{53,66,67} These lie much lower in energy as compared with those for water (sharp features at >9.8 eV). ⁵⁷ In the case of ethanol, the energy splitting of the Rydberg 3p orbitals is very small, and the overlapping transitions in this region give rise to a broad feature between 7.5 and 8.5 eV. ^{58,68–70} A similar broadening is observed with the addition of alkyl groups in the electronic spectra of aldehydes. ⁷¹

A completely different set of spectral features are observed in the 1PA spectrum of liquid methanol, as shown in Figure 1b. In the literature, the location of the first absorption band (1A" ← 1A'), a transition that is clearly observed in the methanol gas-phase spectrum at \sim 6.7 eV, is unclear in the liquid- and solid-phase spectra. Jung et al. 61 proposed that the Isolatedmolecule $1A'' \leftarrow 1A'$ (3s $\leftarrow 2p_z$) transition is blue-shifted by 1.7 and 1.6 eV in methanol and ethanol, respectively, which gives rise to a broad band around 8.3 eV in the absorption spectra of alcohols in the liquid phase. In comparison, Kuo et al. 22 assigned the same 8.3 eV band observed in the 1PA spectra of solid methanol recorded at 10 K to the $2A'' \leftarrow 1A'$ $(3p_x \leftarrow 2p_z)$ transition. Kuo et al. ⁷² also pointed out that given the small oscillator strength of the $1A'' \leftarrow 1A'$ transition observed in the gas phase, it is possible that with a large blue shift the lowest excitation may overlap with stronger features arising from the $2A'' \leftarrow 1A'$ transition (~8.3 eV), and thus is not clearly discernible. Interestingly, by carefully examining their solid-phase MeOH spectra, we noticed a subtle shoulder at \sim 7.4 eV, but the authors did not comment on it at all in their article. We speculate that the shoulder may originate from

the $1A'' \leftarrow 1A'$ transition; however, if our speculation is correct, then the blue shift of the first electronic transition in methanol (\sim 0.7 eV) is significantly less than that reported by Jung et al. (\sim 1.7 eV). In support of our assertion, we note a similar blue shift (0.9 eV) for the first electronic band of water when going from the gas to the condensed phase (7.3 to 8.2 eV), which has been reported by several groups 34,57,59,60 and is shown in Figure 1b. We can expect that a similar line of argument will be true for liquid ethanol as well.

Beyond 9 eV, there is a monotonic increase in the 1PA cross section with the appearance of a shoulder ~9.5 eV. Rydberg transitions with $n \ge 3$ contribute to the higher energy region (> ~9 eV), but because of their overlapping nature, it is difficult to assign each transition separately. 53,72 As can be seen from the low-lying electronic states of the ROH system described above, there is still much to learn about the evolution of the electronic structure in the liquid phase. In this work, 2PA spectroscopy allows us to obtain a better picture of the electronic structure of liquid alcohols and helps us identify the important transitions in the energy range 6.5-10 eV. The key concepts we will be addressing in this Article are as follows: (1) How does the electronic structure of methanol and ethanol deviate from that of water, and what is the effect of an alkyl substitution on the intense transitions in 1PA and 2PA? (2) To what extent do allowed electronic transitions shift and broaden upon solvation? In particular, what happens to the lowest electronic transition? (3) How important are the Rydberg transitions in the liquid phase, and do the transition properties for Rydberg excitations dramatically change upon solvation?

III. METHODS

III.A. Experimental Section. In our experiment, the 7.0– 10.0 eV energy region is accessed by the simultaneous absorption of one deep-UV photon and one UV-visible photon. Both the pump and the probe are overlapped spatially and temporally on a wire-guided gravity jet. Two different pump energies are used: 4.6 (266 nm) and 6.2 eV (200 nm). A white-light continuum from 1.8 (690 nm) to 3.9 eV (315 nm) is used as the probe. The 4.6 eV pump spans a total twophoton energy of 6.7 to 8.5 eV, whereas the 6.2 eV pump extends the spectra to 10.1 eV. The generation of pump and probe beams has been discussed elsewhere.³⁴ At the sample, the 6.2 and 4.6 eV pumps are attenuated to 1.5 and 6 μ J, respectively, with a spatial full width at half-maximum (fwhm) of 400-500 μ m, as determined by the knife-edge technique. The sample is placed at the focal point of the probe continuum (typically 315 < λ_{probe} < 690 nm), where the spatial fwhm's are $60-150 \,\mu\mathrm{m}$ across the continuum spectrum. The spot size and the pulse energy of the pump beam are adjusted to avoid the transient absorption signal from the two-photon ionization of the material.⁷⁴ The wavelength dependence of the spot size of the probe beam is compensated mathematically. The thickness of the liquid jet varies from 40 to 50 μ m, with an estimated 20% error, as measured by the group-velocity delay method. The polarization purity is better than 200:1 across the range of probe wavelengths. The polarization purity of the 4.6 eV pump is better than 70:1, as measured by the extinction of the light through a calcite polarizer, whereas for 6.2 eV pump, the purity is at least 40:1, as measured using a calibrated stack of nine silica plates at the Brewster angle. After passing through the sample, the broadband continuum is dispersed and projected onto a 256-channel silicon photodiode array. Differential

The Journal of Physical Chemistry A

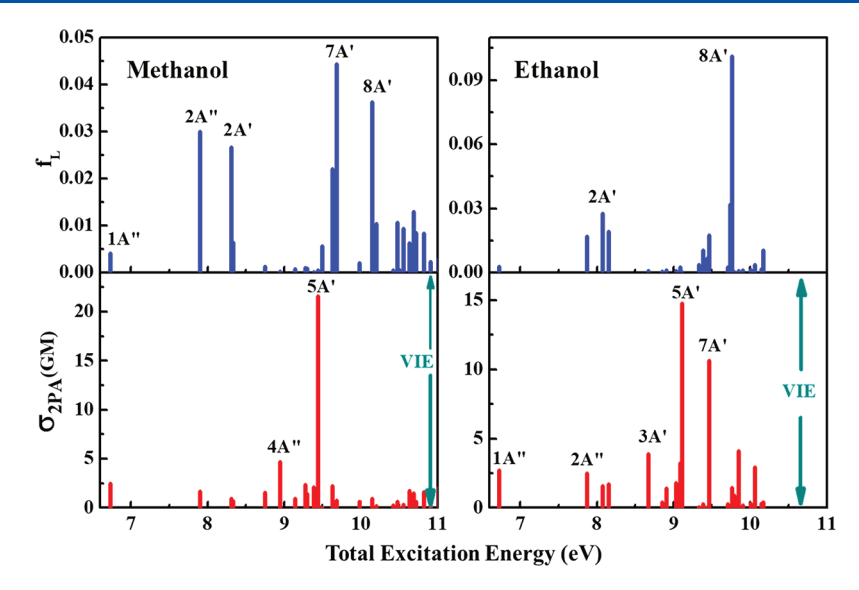


Figure 2. Calculated 1PA and 2PA transitions for methanol and ethanol at the EOM-CCSD/d-aug-cc-PVDZ level of theory. The 2PA cross sections are calculated using a 6.2 eV pump in both cases. The calculated gas-phase vertical ionization energies (VIEs) for methanol and ethanol are also shown.

absorbance $(A_{\text{pump-on}} - A_{\text{pump-off}})$ is recorded for all of the wavelengths in the continuum by measuring the intensity of the probe with and without the pump pulse. The 2PA coefficient β (in cm/W) is calculated as follows

$$\beta = \frac{\ln(10)}{lfE_{\text{pump}}} \int \Delta A_{\text{2PA}}(\tau) d\tau$$
(1)

where τ is the time delay between pump and probe pulses, $\Delta A_{\rm 2PA}(\tau)$ is the differential absorption with the time delay, l is the path length of the sample (in our experiment, it is the thickness of the liquid jet), $E_{\rm pump}$ is the energy of the pump pulse in Joules, and f is the overlap factor accounting for the different spot sizes of pump and probe beams. The signal is integrated from a negative to a positive time delay to eliminate the contribution from the cross-phase modulation signal. The absolute 2PA cross section is calculated by 23

$$\sigma_{\text{2PA}} = \frac{\hbar \omega_{\text{pump}}}{N} \beta \tag{2}$$

where ω_{pump} is the frequency of the pump pulse and N is the number density of the liquid sample. σ_{2PA} is expressed in Goeppert Mayers (1 GM = 10^{-50} cm⁴ s molecule⁻¹ photon⁻¹).

III.B. Computational. The two-photon transition moment is given by the following equations ⁷⁶

$$M_{bc}^{k\leftarrow 0} = -\sum_{n} \left(\frac{\langle k|\mu^{c}|n\rangle\langle n|\mu^{b}|0\rangle}{\Omega_{n0} - \omega_{1}} + \frac{\langle k|\mu^{b}|n\rangle\langle n|\mu^{c}|0\rangle}{\Omega_{n0} - \omega_{2}} \right)$$
(3)

$$M_{bc}^{0 \leftarrow k} = -\sum_{n} \left(\frac{\langle 0 | \mu^{b} | n \rangle \langle n | \mu^{c} | k \rangle}{\Omega_{n0} - \omega_{1}} + \frac{\langle 0 | \mu^{c} | n \rangle \langle n | \mu^{b} | k \rangle}{\Omega_{n0} - \omega_{2}} \right)$$
(4)

where μ is the dipole moment operator, Ω_{n0} is the transition energy between the ground state "0' and the intermediate state "n", and ω_1 and ω_2 are the frequencies used to make two-photon transitions. The rotationally averaged 2PA coefficient is calculated as ^{77,78}

$$\beta = \frac{F}{30} \sum_{a,b} S_{aa,bb} + \frac{G}{30} \sum_{a,b} S_{ab,ab} + \frac{H}{30} \sum_{a,b} S_{ab,ba}$$
 (5)

where S is transition strength matrix

$$S_{ab,cd} = 0.5*(M_{ab}^{0 \leftarrow k} M_{cd}^{k \leftarrow 0} + M_{cd}^{0 \leftarrow k} M_{ab}^{k \leftarrow 0})$$
(6)

and F, G, and H are integer constants that depend on the relative polarization of the two photons. For parallel linearly polarized light, F = G = H = 2; for perpendicular linearly polarized light, F = -1, G = 4, and H = -1.

In the case of degenerate photons, the macroscopic 2PA absolute cross section is calculated as⁷⁹

$$\sigma_{\text{2PA}} = \frac{\pi^3 \alpha a_0^5 (2\omega)^2}{c} \beta S(2\omega, \, \omega_0, \, \Gamma) \tag{7}$$

where α is the fine structure constant, a_0 is the Bohr radius, ω is the photon energy, c is the speed of light, and $S\left(2\omega,\omega_0,\Gamma\right)$ is the line-shape function to account for the spectral broadening.

In the case of nondegenerate photon energies, eq 7 gets slightly modified

$$\sigma_{\text{2PA}} = \frac{2\pi^3 \alpha a_0^5 \omega_{\sigma}^2}{c} \beta S(\omega_{\sigma}, \, \omega_0, \, \Gamma) \tag{8}$$

where ω_{σ} is the sum of the photon energies.

Calculated excitation energies based on a coupled-cluster singles and doubles (CCSD) ground state are generally accurate for both valence and Rydberg states that are primarily single-electron promotions with an error typically around 0.1 to 0.3 eV. Electronically excited states can be calculated at a similar level of theory as the CCSD ground state using equation-of-motion (EOM) methods. For our purpose, we have used the excitation energy (EOM-EE-CCSD) method with the d-aug-cc-PVDZ basis set to calculate the excitation energies for transitions from ground to excited states and the 2PA cross sections associated with each transition in methanol and ethanol. The details of this method have been described elsewhere. The calculated wave functions and the transition energies are used in equations that are formally equivalent to

eqs 3 and 4 for calculating the 2PA transition moments. The orientationally averaged 2PA strength $\beta_{\rm 2PA}$ and macroscopic 2PA cross section $\sigma_{\rm 2PA}$ (in GM unit) are calculated for both parallel and perpendicular polarizations. All calculations are performed using the Q-Chem electronic structure program ⁸³ at the equilibrium geometry of an isolated methanol or ethanol molecule optimized at the CCSD/cc-PVTZ level of theory.

IV. RESULTS AND ANALYSIS

IV.A. Calculation of 2PA Cross-Section. The pointgroup symmetry of isolated methanol and ethanol molecules in their lowest energy conformers is C_s , which has two irreducible representations, A' and A". The 2PA cross sections have been calculated for 42 excited states (up to 11.5 eV) for methanol and 26 states (up to 10.17 eV) for ethanol. The smaller energy range for ethanol is due to the increasing computational cost for the larger molecule. The calculated 2PA cross section with the 6.2 eV pump is higher than that of the 4.6 eV pump. This can be easily understood from eqs 3 and 4; as the energy of one of the photons becomes closer to the excitation energy, the denominator decreases, giving rise to a higher 2PA transition moment. Figure 2 shows the calculated 1PA oscillator strength and the 2PA cross section for parallel polarization at 6.2 eV pump energy. The 1PA oscillator strength has a maximum at a different energy region as compared with the 2PA cross section. This is a result of the different transition moment integrals in 1PA and 2PA spectroscopy.

We also calculated the 2PA polarization ratio corresponding to each transition. For an orientationally averaged sample, a totally symmetric transition has a polarization ratio $\geq 4/3$, whereas in the case of a nontotally symmetric transition, it is \leq 4/3. The ground states for all ROH molecules have A' symmetry. Therefore, a transition to any excited state of A' irreducible representation is totally symmetric, and hence the polarization ratio is >4/3. Conversely, a transition from the ground to any excited state of the A" irreducible representation is a nontotally symmetric transition. Computed results for the total excitation energy $(E_{\rm ex})$, the 1PA oscillator strength $(f_{\rm L})$, the 2PA cross sections for parallel polarization, microscopic $(\beta_{\rm 2PA})$ and macroscopic $(\sigma_{\rm 2PA})$, and the polarization ratio (ρ) corresponding to each transition are presented in Tables 1 and 2 for methanol and ethanol, respectively. The absolute 2PA cross section (σ_{2PA} , in GM) is calculated from the relative 2PA cross section (β_{2PA} , in atomic units) by the equation⁷⁶

$$\sigma^{2\text{PA}} = \frac{2\pi^2 \alpha a_0^5 (\omega_1 + \omega_2)^2 \beta_{2\text{PA}}}{c^* \Gamma^* 10^{-50} * 27.2107} \tag{9}$$

where α is the fine structure constant, a_0 is the Bohr radius in units of cm, Γ is the lifetime broadening (taken to be 0.1 eV), ω_1 and ω_2 are the energies of the two photons in electronvolts, and c is the speed of light in cm/s.

IV.B. Experimental 2PA Spectra and Polarization Ratios. The experimental 2PA spectra of liquid methanol and ethanol are presented in Figure 1c. The absolute 2PA cross section σ_{2PA} is plotted against the total energy of the two photons. Parallel polarization gives rise to a higher cross section throughout the entire spectrum than perpendicular polarization, with a polarization ratio >4/3 above 7.5 eV. This observation alone points to the fact that the spectrum is mainly dominated by totally symmetric transitions, that is, transitions to A' upper states. In the overlapping region, ~8.5 eV, the 6.2 eV pump has a higher 2PA cross section than the 4.6 eV pump

Table 1. Calculated Electronic Transitions of Methanol (EOM-CCSD/d-aug-cc-PVDZ) with 6.2 eV Pump Energy

state	$\frac{E_{\rm ex}}{({ m eV})}$	$f_{\rm L} (\times 10^{-3})$	$eta_{ ext{2PA}}$ (atomic unit) a	$(GM)^a$	2PA polarization ratio $(\rho)^a$	
1A"	6.73	4.0	74	2.5	1.0	
2A"	7.90	30.0	36	1.7	1.3	
2A'	8.31	26.6	18	0.9	1.4	
3A"	8.33	6.4	13	0.7	0.7	
3A'	8.75	1.2	28	1.6	1.8	
4A"	8.95	0.2	80	4.7	1.0	
5A"	9.14	0.8	15	0.9	0.6	
4A'	9.28	1.0	37	2.4	2.1	
6A"	9.30	0.9	22	1.4	1.3	
7A"	9.38	0.1	33	2.1	0.9	
5A'	9.44	0.5	330	21.6	11.2	
8A"	9.49	5.6	0.3	0.02	0.5	
6A'	9.63	22.0	33	2.3	6.7	
7A'	9.68	44.3	11	0.8	1.7	
9A"	9.68	2.3	0.9	0.1	0.9	
10A"	9.98	2.1	9	0.6	1.0	
8A'	10.15	36.3	13	1.0	11.1	
11A"	10.17	2.4	0.1	0.004	0.4	
12A"	10.20	10.4	3	0.2	1.3	
13A"	10.42	0.5	4	0.3	0.9	
9A′	10.47	10.7	8	0.6	5.1	
14A"	10.50	0.7	0.4	0.03	1.1	
^a 6.2 eV pump energy.						

Table 2. Calculated Electronic Transitions of Ethanol (EOM-CCSD/d-aug-cc-PVDZ) with 6.2 eV Pump Energy

state	$\frac{E_{\rm ex}}{({ m eV})}$	$f_{\rm L} \times 10^{-3}$	β_{2PA} (atomic unit) ^a	$(GM)^a$	2PA polarization ratio $(\rho)^a$	
1A"	6.73	2.8	82	2.7	1.0	
2A"	7.87	17.0	55	2.5	1.2	
2A'	8.07	27.6	33	1.6	1.7	
3A"	8.15	19.3	35	1.7	1.2	
3A'	8.67	0.9	70	3.9	6.5	
4A"	8.85	0.6	7	0.4	0.3	
5A"	8.91	1.1	24	1.4	1.3	
6A"	9.03	0.8	30	1.8	1.1	
7A"	9.08	2.6	13	0.8	0.6	
4A'	9.08	0.1	53	3.2	2.1	
5A'	9.11	0.3	242	14.8	12.5	
8A"	9.33	3.7	1	0.1	0.6	
6A'	9.38	10.6	4	0.3	13.8	
9A"	9.44	6.8	1	0.1	0.9	
7A'	9.47	17.6	162	10.7	87.9	
10A"	9.71	2.6	4	0.3	0.9	
11A"	9.74	31.9	3	0.2	1.3	
8A'	9.77	101.1	21	1.5	7.6	
12A"	9.79	0.2	12	0.9	1.2	
9A′	9.85	0.9	58	4.1	10.3	
13A"	9.85	0.2	3	0.2	0.7	
14A"	9.90	1.1	3	0.2	1.1	
15A"	10.01	1.4	5	0.3	1.3	
10A'	10.06	3.7	40	3.0	9.8	
16A"	10.15	1.7	4	0.3	1.0	
11A'	10.17	10.5	5	0.4	33.4	
^a 6.2 eV pump energy.						

due to preresonant enhancement, as expected from eqs 3 and $4.^{34}$ The comparison of $\sigma_{\rm 2PA}$ values between our study and the

literature is summarized in Table 3. The difference in absolute values at 9.4 eV likely originates from the fact that 264 nm

Table 3. Absolute 2PA Cross Sections (in GM) for Parallel Polarization at 7.14 and 9.4 eV for Methanol and Ethanol

2PA energy (photon combination, nm)	7.14 eV (266/500) ^a	7.14 eV (347/347) ^b	9.4 eV (200/387) ^c	9.4 eV (264/264) ^d
methanol	0.15 ± 0.06	0.32	5.1 ± 2.0	1.7 ± 0.2
ethanol	0.30 ± 0.12	0.45	7.6 ± 3.0	3.1 ± 0.3

^aThis study: 266 nm pump and 500 nm probe (selected from the continuum). ^b2PA coefficient (β , in cm/GW) taken from ref 16. Converted to 2PA cross section (σ , in GM) using the following parameters: $M_{\rm methanol} = 32$ g/mol, $\rho_{\rm methanol} = 0.791$ g/cm³, $M_{\rm ethanol} = 46$ g/mol, and $\rho_{\rm ethanol} = 0.785$ g/cm³. The error was not reported by the author. ^cThis study: 200 nm pump and 387 nm probe (from the continuum). ^d2PA coefficient (β , in cm/GW) taken from refs 17 and 18 converted to 2PA cross section (σ , in GM) using the parameters shown in footnote b. 10% error was reported by the authors.

photons are further away from resonance. At 7.1 eV, the absolute values reported here are in reasonable agreement with the literature

Figure 3 shows the polarization ratio as a function of total 2PA energy for both 4.6 and 6.2 eV pumps. The polarization ratio is ~3.0 at 10.0 eV and decreases to ~2.0 at 8.3 eV. Such a trend is preserved in the lower energy region covered by the 4.6 eV pump, where the polarization ratio decreases from \sim 2.75 at 8.5 eV to \sim 1.0 at 7.0 eV. This observation suggests that the contribution from nontotally symmetric transitions becomes more prominent in the lower energy region, that is, the ground to the 1A" state $(3s \leftarrow 2p_z)$ and to the 2A" state $(3p_x \leftarrow 2p_z)$. As can be seen in Figure 3, transitions to equivalent states in water also have low polarization ratios.³⁴ The overall trend of methanol polarization ratio bears more resemblance to water than higher alcohols, where the polarization ratio spectrum is rather flat. (The 2PA spectra of propanol and butanol and the polarization ratio are shown in Figures S1 and S2.)⁸⁷ For example, in ethanol, the polarization ratio shows less variation within our experimental spectral range; the ratio is ~3.0 in the lower energy region and maintains a value >2.5 throughout. This suggests that transitions to the excited states of A" symmetry (nontotally symmetric transition) have a relatively small cross section in the 2PA spectra of ethanol, even in the lower energy region. One explanation is that the ethyl group has a larger effect on reducing the molecular symmetry. Alternatively, unlike methanol, the electronic structure in higher alcohols is less

dominated at lower energy by transitions involving oxygencentered orbitals and thus increasingly deviates from water.

We observe that in the overlapping region, the polarization ratio with a 4.6 eV pump is higher than that with a 6.2 eV pump for methanol, whereas in the case of ethanol, they are almost the same. For both alcohols, we identify from the electronic structure calculations that transitions to 2A' and 3A" excited states are most likely to contribute to the overlapping region of the spectra. For methanol, when going from 4.6 to 6.2 eV pump energy, the theoretically predicted polarization ratio decreases by a factor of 1.6 and 1.9, respectively, for these two states (Table 1 and Table S1), whereas for ethanol, the polarization ratio increases by a factor of 1.3 for the 2A' state and decreases by a factor of 1.1 for the 3A" state (Table 2 and Table S2) when a higher energy pump photon is used. These two competing factors cancel out, resulting in an identical polarization ratio of EtOH in the overlapping region for both 4.6 and 6.2 eV pump excitation.

We can compare the polarization ratio at 7.92 eV to that obtained by Rasmusson et al.⁸⁸ using an identical photon combination (Table 4). Our experimental values are close to,

Table 4. Linear Polarization Ratio at 7.92 eV (266 + 380 nm) for Methanol and Ethanol

	methanol	ethanol
this work ^a	1.9	3.2
Rasmusson ^b	1.5	3.1

^a266 nm pump and 380 nm probe (selected from the continuum). ^bData taken from ref 88.

but consistently higher than, their values. This discrepancy may be explained by the fact that the measurement by Rasmusson et al. 88 includes a considerable amount of background transient absorption signal, most likely due to two- (pump-) photon ionization of the solvent. Because the absorption due to photoionization photoproducts (e.g., solvated electrons) is isotropic, the background signal will reduce the 2PA polarization ratio. In light of this, it is worthwhile to stress that using the appropriate pump irradiance to eliminate the transient absorption (pump-probe) signal is essential for accurately measuring 2PA polarization ratios.

V. DISCUSSION

V.A. Characterization of Excited States: 1PA versus 2PA Spectra. An initial characterization of the excited states can be gleaned from a natural transition orbital (NTO) analysis, identifying the orbitals participating in a particular

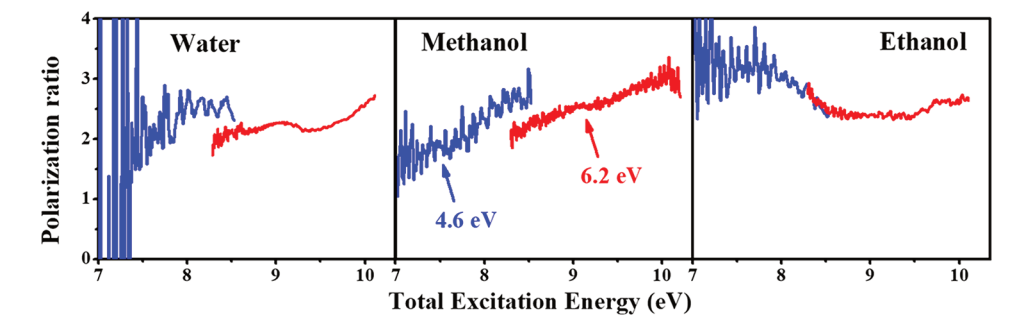


Figure 3. Experimental polarization ratio (ρ) for water, methanol, and ethanol plotted against the total excitation energy with (blue) 4.6 and (red) 6.2 eV pumps.

The Journal of Physical Chemistry A

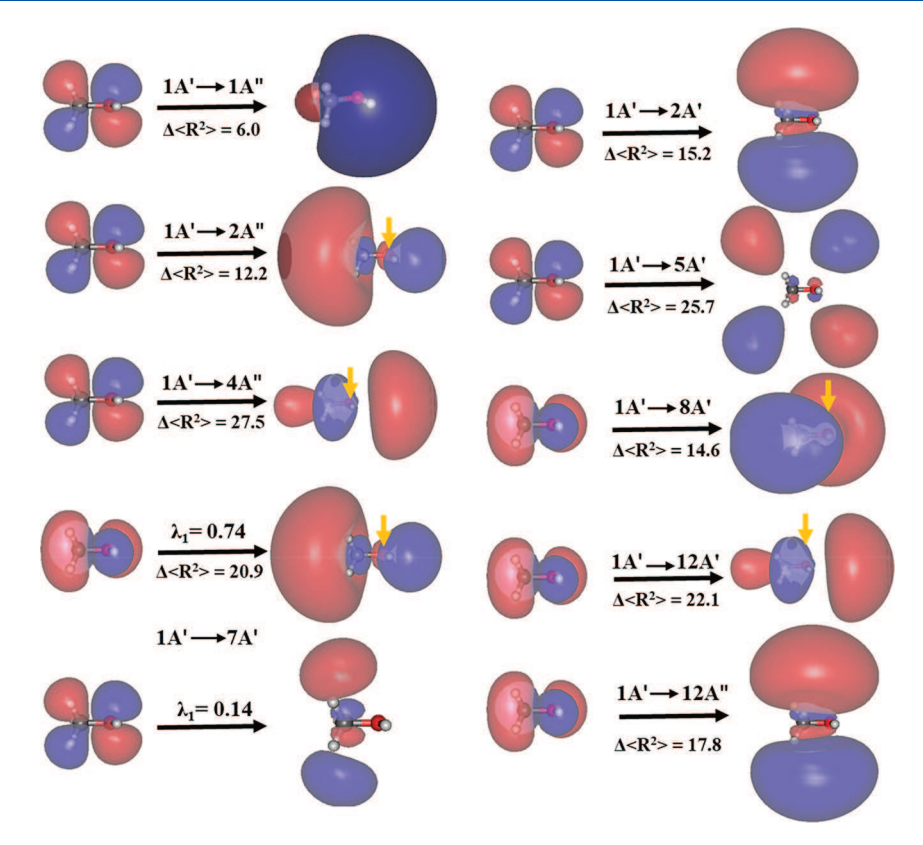


Figure 4. NTOs corresponding to the strong 1PA and 2PA transitions in methanol. An isovalue of 0.015 is used for rendering orbital surfaces. The yellow arrow points to the position of the oxygen atom.

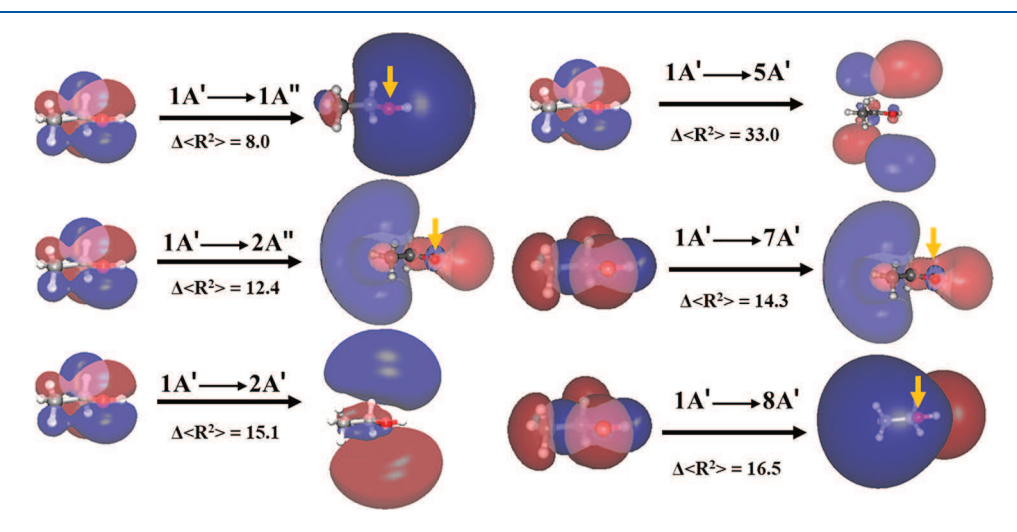


Figure 5. NTOs corresponding to the strong 1PA and 2PA transitions for ethanol. An isovalue of 0.015 is used for rendering orbital surfaces. The yellow arrow points to the position of the oxygen atom.

transition. The NTOs for important transitions in isolated methanol and ethanol are displayed in Figures 4 and 5, respectively. Several key parameters $^{89-91}$ related to the excited-state wave functions are reported in Table 5. They include the absolute mean separation $|\overrightarrow{d_{h\to e}}|$ between the average positions of electron and hole, the size of the electron (σ_e) and hole (σ_h) , and the change in the size of the wave function following the excitation, $\Delta < R^2 > .^{31}$ For transitions to valence states, $\Delta < R^2 >$ is small, but a large value is expected for transitions to Rydberg states. The NTO participation ratio $(PR_{\rm NTO})$, as shown in eq 10, indicates how many significant NTO pairs are needed to describe a transition.

$$PR_{NTO} = \frac{\left(\sum_{i} \lambda_{i}\right)^{2}}{\sum_{i} \lambda_{i}^{2}}$$
(10)

where λ_i is the weight of a respective configuration obtained by the singular value decomposition of the transition density matrix. 90,91

The first distinct difference between the 1PA and 2PA spectra of methanol is the presence of a shoulder in the 2PA spectrum at ~ 7.6 eV but not in 1PA, as shown in the inset of Figure 1b,c. This can be readily explained by comparing the calculated 1PA and 2PA transition strengths in Figure 2. In the 6.5-9 eV region, the ratio of the 1PA oscillator strengths for

Table 5. Key Parameters from NTO Calculations for Methanol and Ethanol^a

state	$\frac{E_{\mathrm{ex}}}{(\mathrm{eV})}$	$ \overrightarrow{d_{\mathrm{h} \to \mathrm{e}}} $ (Å)	$\binom{\sigma_{ m e}}{({ m \AA})}$	$\sigma_{ m h} \ ({ m \AA})$	$\sigma_{ m e} - \sigma_{ m h} \ (m \AA)$	PR_{NTO}	$\Delta < R^2 >$
methanol							
1A''	6.73	1.27	2.51	1.18	1.33	1.01	6.0
4A"	8.95	2.23	4.86	1.20	3.66	1.01	27.5
5A'	9.44	0.55	5.33	1.22	4.11	1.02	25.7
2A''	7.90	2.05	3.42	1.25	2.17	1.01	12.2
2A'	8.31	0.74	4.19	1.22	2.97	1.01	15.2
7A'	9.68	1.78	4.62	1.34	3.28	1.4	20.9
8A'	10.15	0.42	4.16	1.33	2.83	1.02	14.6
ethanol							
1A"	6.73	1.44	2.58	1.22	1.36	1.01	8.0
2A"	7.87	1.92	3.69	1.34	2.35	1.03	12.4
3A'	8.67	1.66	2.90	1.42	1.48	1.04	8.8
5A'	9.11	0.71	6.06	1.29	4.77	1.03	33.0
7A'	9.47	1.63	4.02	1.49	2.53	1.16	14.3
2A'	8.07	0.71	4.20	1.29	2.91	1.01	15.1
8A'	9.77	0.5	4.52	1.49	3.03	1.05	16.5

^aExcitations to the states labeled in bold and italic are bright in 2PA and 1PA, respectively.

 $2A'' \leftarrow 1A'$ and $1A'' \leftarrow 1A'$ transitions is 8, whereas the intensity ratio of the same transitions is 0.7 in the 2PA spectrum. Thus the relative intensities of the two transitions are predicted to be different by a factor of 11 between the 1PA and 2PA spectra. As a result, the lowest excitation band $(1A'' \leftarrow 1A')$ centered at 6.7 eV should be revealed in the 2PA spectrum, whereas the existence of this first transition is buried in the tail of the strong band centered around 7.9 eV in the 1PA spectrum.

Another interesting point is observed from the theoretical calculation of 1PA and 2PA for methanol. In the 2PA spectrum, the $5A' \leftarrow 1A'$ transition has the highest cross section, whereas the $7A' \leftarrow 1A'$ transition accounts for the highest oscillator strength in the 1PA spectrum. Clearly, different transitions are favored in 2PA than in 1PA, which is in line with the different selection rules. In 2PA, the $5A' \leftarrow 1A'$ transition is mainly governed by the promotion of the electron from the 2a" orbital (HOMO) to the 5a" orbital (LUMO+10), as shown in Figure 4. The HOMO in methanol mainly consists of the nonbonding (out-of-plane) $O(2p_z)$ mixed with $C(2p_z)$. The 5a'' orbital is the $O(3p_z)$ mixed with $C(3p_z)$. Therefore, the $5a'' \leftarrow 2a''$ promotion, in essence, is a $p_z - p_z$ transition on each atom, a transition with no change in orbital angular momentum that is unfavorable in 1PA but strongly allowed in 2PA. Equivalently, one can consider these molecular orbitals centered between the carbon and oxygen, and because both resemble d orbitals around this center, there is no change in angular momentum. On the contrary, the $7A' \leftarrow 1A'$ transition, which shows the highest 1PA oscillator strength, can be described by two participating NTO pairs. The relative contribution (λ) of each NTO pair³¹ is shown in Figure 4. The NTO pair that has the major contribution toward this transition involves exciting an electron from orbital 7a' (HOMO-1) to 14a' (LUMO+8). The HOMO-1 mostly has the (in-plane) character of $O(2p_v)$ mixed with $C(2p_v)$ and 1s orbitals of the methyl hydrogen atoms. The 14a' orbital mainly has "3s" Rydberg character, so the 14a' \(
4 7a' \) promotion is a 3s \leftarrow 2p_v type transition with a ± 1 change in angular momentum that is favorable for 1PA. For ethanol, the

 $5A' \leftarrow 1A'$ transition has the highest 2PA cross section and originates from a p_z-p_z transition like methanol, whereas the $8A' \leftarrow 1A'$ transition has the highest 1PA oscillator strength and involves promoting an electron from the in-plane $2p_y$ orbital to the Rydberg 3s orbital. This observation leads us to conclude that although the transitions in methanol and ethanol are mainly governed by the molecular selection rules applied to the C_s point group, transitions involving Rydberg orbitals can be realized by merely considering the atomic selection rule.

V.B. Comparing 2PA Spectra of Water, Methanol, and Ethanol. A comparison of the 2PA spectrum of H₂O with those of MeOH and EtOH reveals several significant points. The first 1PA band of water is very weak in 2PA, as reported by Elles et al.,³⁴ but in the case of MeOH and EtOH, this transition gains intensity. This can be reconciled by considering the contribution of multiple atoms to the relevant molecular orbitals in alcohols. It has been shown by experimental and theoretical studies 92-94 that the HOMO of methanol is a combination of 70% oxygen p character and 30% carbon p and hydrogen s characters. Our calculations also confirm these results. Furthermore, the LUMOs of the alcohols also have contributions from both oxygen and carbon. 53,58,95 As a result, the atomic selection rules that describe the electronic transitions in water surprisingly well are now relaxed, and the molecular selection rule in the C_s framework starts to play an important role in making the lowest energy $3s \leftarrow 2p_z$ transition acquire a considerable 2PA cross section. This effect helps bring the 2PA threshold energy down to ~6.9 eV in methanol and ethanol compared with that of water (\sim 7.8 eV), as shown in Table 6. An important consequence of the higher 2PA threshold in water is an almost 1 eV broader window for the 2PA spectroscopy of dissolved solutes compared with the alcohols.

Table 6. 1PA and 2PA Absorption Thresholds of Liquid Water, Methanol, and Ethanol (in eV)

	water	methanol	ethanol
1PA(99%T)	~6.4 ^a	5.6 ^b	5.6 ^b
$2PA(99\%T)^{c}$	7.8	6.9	6.9

"Data taken from ref 96. The extinction coefficient at 6.4 eV is $\sim\!2.25\times10^{-4}~\rm M^{-1}~cm^{-1}$, corresponding to a transmission slightly greater than 99% in a 0.1 cm cell. ^bData taken from ref 97. The thresholds were the energies where the transmission of the liquid was $\sim\!99\%$ in a 0.1 cm cell. ^cThis study. The 2PA thresholds are the energies where the transmission of the probe is $\sim\!99\%$ (equivalent to absorbance of $\sim\!4$ mOD) in a 0.1 cm path length with a peak irradiance of the 267 nm pump pulse = $\sim\!100~\rm GW/cm^2$. This is estimated based on the energies where the absorbance was $\sim\!0.2~\rm mOD$ with a $\sim\!50~\mu m$ path length.

It was shown in the case of water³⁴ that the transition from the ground state to the 3^1A_1 excited state accounts for the highest cross section below ~11 eV in the 2PA spectrum. This transition $(2b_1 \leftarrow 1b_1)$, situated at 10.23 eV, involves promoting an electron from the $2p_z$ orbital of oxygen to the $3p_z$ orbital (z axis is out of plane). For both MeOH and EtOH, the $5A' \leftarrow 1A'$ transition shows the maximum 2PA cross section, and they too are due to $3p_z \leftarrow 2p_z$ excitation. This means that substituting one of the hydrogens in water by a methyl or an ethyl group does not significantly change the nature of the dominant transition in this region of the 2PA spectrum. As shown in Table 5, the $\Delta < R^2 >$ value for this

transition is quite large for both methanol and ethanol (25.7 and 33.0 Å², respectively), reflecting the diffuse $3p_z$ orbitals. Thus totally symmetric transitions to Rydberg-like states dominate the 2PA spectra of water and alcohols.

V.C. Simulation of 2PA Spectrum. Simulating fully condensed-phase 2PA spectra for an extended liquid, just as for 1PA electronic spectra, is a state-of-the-art problem in electronic structure theory. 92-96 Although computations that accurately include the influence of the environment are possible for solutes, 98-103 the quantum-mechanical treatment of a large number of solvent molecules, without edge effects or deficiencies in TD-DFT, is beyond the scope of the current electronic structure. Instead, we calculate the 2PA properties of the isolated gas-phase molecule as a guide for interpreting the spectroscopy of the liquid. Considering the single molecule as a perturbed central chromophore has been shown to be a reasonable starting point for water.³⁴ There are several effects that are important to consider in translating gas-phase calculations to describe the liquid phase, including the shifting of transition energies due to local environment around (or specific interactions with) the central molecular chromophore and the energy broadening of each transition. An important consideration is the fate of Rydberg orbitals in a condensed medium. 39,47,104 A potential problem is that different excited states are likely to behave differently upon solvation.

We start with the excitation energies and 2PA cross sections for transitions to the set of higher excited states obtained from the EOM-CCSD calculations, as described in Figure 2 and Tables 1 and 2. A simulation of the parallel 2PA spectra of methanol with 4.6 eV pump is shown in Figure 6a,b. States up

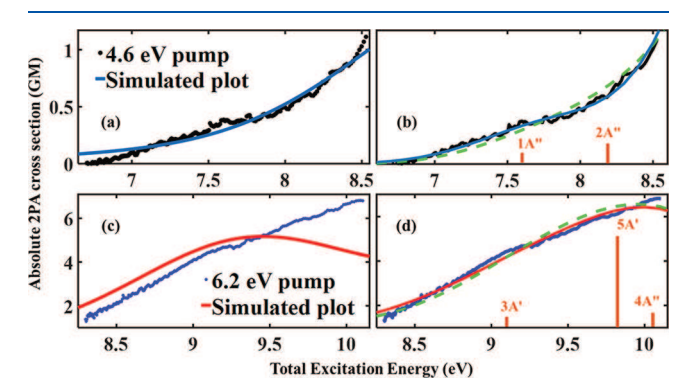


Figure 6. (a) Simulation of the 4.6 eV pump 2PA spectrum using EOM-CCSD transition energies and strengths. The transition widths are 2.0 eV fwhm. (b) Result obtained by applying a 0.9 eV blue shift to the lowest $1A'' \leftarrow 1A'$ transition. The transition widths are 1.1 eV fwhm. (c) Simulation of the 6.2 eV pump 2PA spectrum using the EOM-CCSD results. The transition widths are 1.4 eV fwhm. (d) Simulated spectrum obtained by blue-shifting the first transition by 0.9 eV. $4A'' \leftarrow 1A'$ and $12A' \leftarrow 1A'$ transitions are blue-shifted by 1.2 eV, and all other transitions are blue-shifted by 0.33 eV. Peaks are modeled with Gaussian fwhm's of 1.0 and 1.75 eV. Green dotted lines correspond to an identical simulation, except $2A' \leftarrow 1A'$ and $12A'' \leftarrow 1A'$ transitions are now blue-shifted by 1.2 eV.

to 10A'' (9.99 eV) have been included in this simulation, and the resulting spectrum in Figure 6a is obtained directly from the calculated results without any adjustments to intensities or positions. Normalized Gaussians are centered around the calculated excitation energies, and each transition is, somewhat arbitrarily, given a fixed Gaussian width, \sim 2.0 eV fwhm. The simulation accurately predicts the mostly featureless rise of the

2PA cross section with increasing energy up to \sim 7.5 eV but fails to reproduce the more subtle features of the experimental spectra.

The simulation in Figure 6b is obtained by keeping the calculated positions and cross sections of all electronic transitions unchanged except for applying a 0.9 eV blue shift to the position of the first electronic transition, $1A'' \leftarrow 1A'$. The justification for such a large shift comes from the previous work,³⁴ where there is good agreement that the first electronic transition in water blue shifts by 0.9 eV when going from gas to liquid. 59,67 For both water and methanol, the first transition is due to the promotion of an electron from the 2pz to the 3s Rydberg orbital of oxygen, so it is reasonable to expect such a blue shift in methanol, too. Interestingly, shifting the energy of the lowest transition alone is sufficient to reproduce most of the subtle curvature in the experimental 2PA spectra of methanol in this spectral region, as shown in Figure 6b. The simulation gives even better agreement by reducing the bandwidth to 1.1 eV fwhm. Such a blue shift of low-n Rydberg transitions is consistent with the observation by Vigliotti et al. for NO in rare-gas matrices.⁵¹ We compare this reduced bandwidth and 0.9 eV shift of the lowest transition energy with the 1PA spectrum of methanol below.

It is worth mentioning that the calculated absolute 2PA cross sections (σ_{2PA}), as in Tables 1 and 2, are different from the experimental values by a factor of "3" for methanol and "1.4" for ethanol. Such discrepancy in absolute magnitude may result from both the uncertainty in the experimental parameters, such as the laser spot size, and the simplicity of the theoretical spectral model. Therefore, a free scaling parameter is applied to match the overall spectral intensity in the simulation with experiment.

Simulations of the parallel 2PA spectra with the 6.2 eV pump are shown in Figure 6c,d. States up to 12A' (10.91 eV) have been included in this simulation. As before, the simulation shown in Figure 6c is obtained by using the calculated EOM-CCSD results without any adjustment in the position or the cross section of any transition. The simulation does not accurately reproduce the experimental intensity distribution above ~ 9.3 eV. Whereas the experimental spectrum shows a monotonic rise in the cross section from 8.3 to 10.2 eV, the simulation shows a maximum at ~ 9.4 eV, with the cross section decreasing at higher energy. The decreasing cross section at higher energy in the simulation is not simply a result of truncating the calculations because the calculated transition energies extend 0.8 eV above the energy range shown.

To understand how the electronic energy levels are shifted from the gas to the condensed phase, the absorption spectra of solid methanol are a good starting point. Only three Gaussians are necessary to reproduce the experimental absorption spectrum of solid methanol at 10 K, as reported by Kuo et al.⁷² The first two Gaussians are centered at around 8.45 and 10.5 eV, with bandwidths of 1.25 and 3 eV, respectively. We followed the same procedure to fit the liquid 1PA spectrum of methanol measured by Jung et al.⁶¹ The simulation of the liquid spectrum also requires three Gaussians, centered at 8.15, 10.05, and 11.66 eV, with bandwidths of 0.97 and 2.07 eV, respectively, for the first two Gaussians. Comparing the peak positions obtained by fitting the experimental solid- and liquidphase 1PA spectra of MeOH to the results of our gas-phase EOM-CCSD calculations, as shown in Figure 2 (top), clearly reveals that in both cases all strong transitions in 1PA are blueshifted. Another important result revealed by this fitting exercise is that the Gaussian width increases by almost a factor of 2 to 2.5 from the lower to the higher energy region of the spectra. An improved simulation of the experimental 2PA spectra can certainly be done by incorporating all of these factors. Moreover, careful inspection of the NTO plots for MeOH shown in Figure 4 reveals that the upper orbitals of the $4A'' \leftarrow 1A'$ and $12A' \leftarrow 1A'$ transitions are identical and have significant Rydberg 3s character centered on oxygen. The Rydberg character is similar to the upper orbital of the first transition $(1A'' \leftarrow 1A')$. Therefore, it follows that $4A'' \leftarrow 1A'$ and $12A' \leftarrow 1A'$ transitions will have a similar blue shift upon solvation. We account for these effects in the simulation of the 6.2 eV 2PA spectrum in Figure 6d, where the first transition $(1A'' \leftarrow 1A')$ is blue-shifted by 0.9 eV, the $4A'' \leftarrow 1A'$ and $12A' \leftarrow 1A'$ transitions are blue-shifted by 1.2 eV, and all other transitions are given a uniform blue shift of 0.33 eV (see below). States up to 9 eV are given a similar Gaussian width (\sim 1.0 eV), and beyond that a different Gaussian width (\sim 1.75 eV) is applied for the rest of the transitions.

Now, to provide some confidence as to how reasonable the shift of the electronic states and the adoption of two different bandwidths are, we simulate the liquid 1PA spectra using the gas-phase 1PA oscillator strengths calculated by the EOM-CCSD method and keep the same set of contraints used for the 2PA simulation. As shown in Figure 7a, the simulation

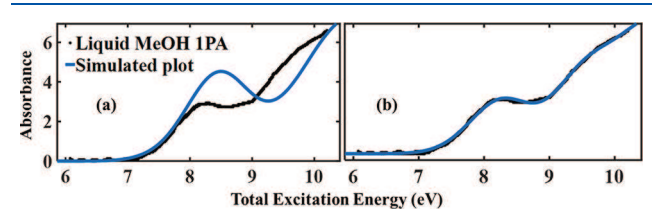


Figure 7. Simulation of the 1PA spectrum of liquid MeOH: (a) by using the same parameters as those used to simulate Figure 6d and (b) with selected additional transitions $(2A' \leftarrow 1A'$ and $12A'' \leftarrow 1A')$ given different blue shifts as mentioned in the text.

does not immediately reproduce the experimental 1PA spectrum well, but if we simply allow a different blue shift (1.2 eV) for the $2A' \leftarrow 1A'$ transition, then the experimental spectra and the simulation show a remarkable resemblance. Moreover, as shown in Figure 4, the upper orbital corresponding to the $12A'' \leftarrow 1A'$ transition is the same as that of the $2A' \leftarrow 1A'$ transition. Hence a similar blue shift is expected for the $12A'' \leftarrow 1A'$ transition as well. The justification for a larger shift for the $2A' \leftarrow 1A'$ and $12A'' \leftarrow 1A'$ transitions is discussed later.

Keeping all of these factors in mind, the revised 1PA simulation in Figure 7b includes blue shifts of 0.9 eV for the lowest transition, 1.2 eV for the transitions to 2A', 4A", 12A", and 12A', and 0.33 eV for all other transitions. States up to 9 eV have a Gaussian width of 1 eV, and the rest are given a Gaussian width of 1.75 eV. Now, to check the consistency, these parameters are used to resimulate the 2PA plots. The revised 2PA simulations are shown as the green dotted lines in Figure 6b,d, and they are little changed from the previous simulations (red, blue). This again reflects the complementarity of the transitions having significant intensity in 1PA versus 2PA spectra. The simulation procedure clearly establishes our hypothesis that the first electronic excited state blue shifts from the gas to the liquid phase; the blue shift (0.9 eV) is almost

half of that predicted by Jung et al. 61 (1.7 eV). This smaller blue shift provides an explanation for the shoulder at \sim 7.4 eV that we observed in the solid-phase methanol spectrum measured by Kuo et al. 72

We have previously shown that the polarization ratio is a sensitive tool to analyze experimental 2PA spectra, especially when there are a number of overlapping transitions in the spectral range.³⁴ If there is a single transition that dominates the experimental 2PA spectrum, then the polarization ratio has a constant value. Any change in the polarization ratio in the spectral region signifies contributions from additional transitions. For methanol, as we have noted, the polarization ratio increases monotonically from 7 to 10 eV. Figure 8a,b shows

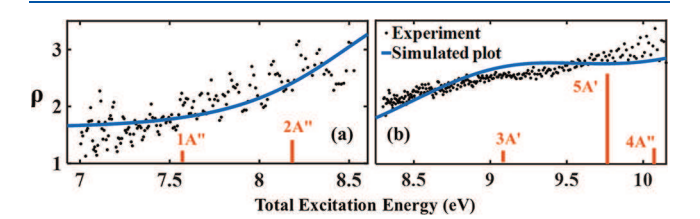


Figure 8. Simulation of the polarization ratio (ρ) spectrum of methanol for (a) 4.6 and (b) 6.2 eV pumps. The excitation energies have been shifted and use two different Gaussian widths, as described in the text.

the simulated polarization ratio for 4.6 and 6.2 eV pump photons, respectively, using polarization-dependent intensities for each transition from the EOM-CCSD calculations (eq 5). Thus we use the simulation parameters reported above to simultaneously reproduce both the parallel and perpendicular polarized 2PA spectra as well as the 1PA spectrum of liquid methanol. Thus the polarization simulation helps us evaluate the degree of shifting of the electronic states and their broadening upon solvation. It should be kept in mind that the reported shift and broadening of the electronic states are only meant to capture the overall picture of the molecule upon solvation. The shift and the broadening of each individual excited state likely differ; the determination of these properties from first-principles is beyond the scope of this Article.

In the case of ethanol, the calculation of the 2PA cross section is limited to states up to 10.15 eV. To accurately reproduce the rising edge of the experimental spectrum beyond 10 eV, a Gaussian centered around 10.95 eV is added to the simulation (with a polarization ratio of 2). Every calculated state is given a uniform blue shift of 0.2 eV, except for the first state, which is given a blue shift of 0.9 eV. States up to 9 eV are broadened by 0.7 eV, and the rest have a broadening of ~2.6 eV. We suspect that this larger width for the higher transitions (as well as the arbitrary additional peak) is necessary simply because of the truncation of excitations computed for EtOH. The difference, however, in the lower energy transition line width is significant; methanol has ~50% broader transitions than ethanol. To rationalize this difference in the lower energy part of the spectrum, we refer readers to the partial radial distribution functions, $g_{OO}(r)$, obtained by molecular-dynamics (MD) simulations of liquid methanol and ethanol at room temperature (298 K). As a general trend, the first maxima corresponding to $g_{OO}(r)$ function appear at the same position in both methanol and ethanol, but the height of the maximum is greater in the case of ethanol, 107 even though the molecular number density of methanol at 298 K (1.48 \times 10⁻² molecule ${\rm \AA}^{-3}$) is higher than that of ethanol (1.03 \times 10⁻²

molecule Å⁻³).¹⁰⁷ This leads to the conclusion that at room temperature, ethanol is more structured than methanol; for an identical character electronic transition, this should give rise to a smaller inhomogeneous transition line width in the case of ethanol, exactly as required in our spectral simulation.

The simulated 2PA spectrum and the polarization ratio of EtOH are shown in Figure 9. Although our simulation

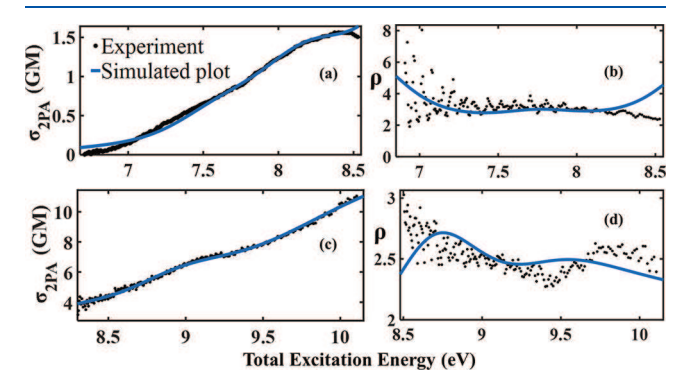


Figure 9. Simulation of parallel 2PA spectra of ethanol for (a) 4.6 and (c) 6.2 eV pumps. Simulation of ethanol polarization ratio (ρ) for (b) 4.6 and (d) 6.2 eV pumps.

reproduces the experimental 2PA spectra with 4.6 and 6.2 eV pumps quite well, it fails to capture some subtle features in the polarization ratio. For example, the simulation does not reproduce the slight dip in experimental polarization ratio around 9.5 eV. This again emphasizes the fact that unlike the absolute 1PA and 2PA spectra, the 2PA polarization ratio is an extremely sensitive experimental quantity; an accurate simulation of the polarization ratio requires knowledge of the shift and broadening of every transition. Nevertheless, the overall trend in the polarization ratio helps us determine the transitions that contribute the most to the experimental 2PA spectra, especially when there are several overlapping transitions.

Finally, we return to the fate of Rydberg transitions upon solvation. Although several experimental 49-52,55,56,104,108 and theoretical works 45,46 have been carried out to address this problem, the issue of Rydberg states in the condensed phase is very much an open question; however, our simulations of the spectra for liquid methanol and ethanol provide important clues based on the magnitudes of the shifts assigned to different electronic transitions from the isolated-molecule reference. For both alcohols, the first excited state originating from a $3s \leftarrow 2p_z$ transition requires blue shifting by a relatively large 0.9 eV; we speculate that this is because the Rydberg 3s orbital is more compact than the higher-lying and higher angular momentum Rydberg orbitals, which experience particularly large Pauli repulsion.³⁴ This observation is consistent with the blue shifting of low-n Rydberg transitions for NO in rare-gas matrices observed by Vigliotti et al.⁵¹ These authors comment that the n = 1 exciton, that is, the exciton obtained following an excitation to the lowest Rydberg orbital, is somewhat different from the remaining states $(n \ge 2)$ because it has a smaller characteristic radius than the solidstate unit cell.⁵¹ In methanol, we applied a large blue shift to transitions to the 2A', 4A", and 12A' states, in addition to the first excited state. (The $12A'' \leftarrow 1A'$ transition was also shifted by ~ 1 eV to be consistent, as the upper orbital for this transition is the same as the $2A' \leftarrow 1A'$ transition.) Inspecting the NTO plots corresponding to $4A'' \leftarrow 1A'$ and $12A' \leftarrow 1A'$ transitions, we notice that in both cases the upper orbitals also have a significant amount of "s" character centered on oxygen. These transitions have considerable 2PA cross section for an isolated molecule, and shifting these states is absolutely necessary to reproduce the experimental 2PA spectra and the polarization ratio in the liquid. Because the oxygen atom acts as a H-bond acceptor, it makes sense that charge density centered on oxygen will face enhanced Pauli repulsion from the closer-coordinated solvent, leading to a larger blue shift upon condensing. On the contrary, the $2A' \leftarrow 1A'$ transition also needs to be blue-shifted by ~1 eV to simulate the liquid 1PA spectrum of methanol. NTO plots show that the upper orbitals corresponding to these transitions are of "3p" type, where "3p" orbitals centering on carbon and oxygen constructively interfere with each other. Whereas we cannot currently rationalize this large shift, interestingly, such a large shift is not required for the similar transitions in ethanol. To understand the latter point, we refer to Table 5. NTO calculations provided a number of excitation characteristics, including the sizes of the electron (σ_e) and hole (σ_h) , the absolute mean separation between the average positions of the electron and hole $(|d_{h\rightarrow e}|)$, and the change in the size of the wave function following the excitation ($\Delta < R^2 >$). In going from methanol to ethanol, for a transition involving similar lower and upper orbitals (as can be seen from NTO plots), all of these parameters $(\sigma_e, \sigma_h, |d_{h\rightarrow e}|, \Delta < R^2 >)$ increase in magnitude, which is consistent with the increase in the size of the molecule. The $2A' \leftarrow 1A'$ transition, however, does not follow this trend. The size of the electron (σ_a) corresponding to this transition is almost the same in both methanol and ethanol, 4.19 and 4.20 Å, giving rise to the $\Delta < R^2 >$ values of 15.2 and 15.1 Å^2 and the mean electron—hole separation $|d_{\text{b}}|$ of 0.74 and 0.71 Å, respectively. This leads to a relatively smaller Pauli repulsion for the Rydberg electron in ethanol than methanol, leading to a smaller blue shift for ethanol.

In ethanol, the spectrum can be reproduced from the isolated-molecule calculation simply by blue-shifting all of the states equally by 0.2 eV, except the first transition, which, as for water and methanol, has a larger blue shift (0.9 eV here). Unlike methanol, no corrective shift is needed for any other transition, even for the transitions having an apparent "s" character on the oxygen atom. We suspect that is due to the increase in the size of the alkyl group, where increasing carbon orbital character is involved in the upper state. Only the first transition preserves the majority O(3s) character. For transitions involving higher Rydberg states, the generalized blue shift for ethanol (relative to gas phase) is less than that for methanol (0.33 eV). These Rydberg states of ethanol are more delocalized over the molecular framework, and from Table 5, we can see that they also reach further into the solvent. Such diffuseness results in less shielding of the cationic core in ethanol, leading to greater polarization stabilization. Moreover, a decrease in the number density going from methanol to ethanol contributes to the smaller Pauli repulsion of the excited electrons to the Rydberg orbitals. 109 These two effects explain a smaller blue shift in ethanol as compared with methanol.

Alcohols have proven to be ideal candidates for studying the effect of solvation on Rydberg transitions, as their excited states in the gas phase are mainly of Rydberg type because of

the lack of π bonding in these molecules. In the case of both alcohols studied here, the Rydberg states are central in characterizing the one- and two-photon spectra, even at the lowest transition energies. For example, our calculations show that the highest cross-section 2PA transition $(5A' \leftarrow 1A')$ involves dominant Rydberg character. A related transition can be identified in the liquid 2PA spectrum based on the high polarization ratio that is required to reproduce the experimental 2PA polarization spectrum. It is fascinating that knowledge of the isolated-molecule Rydberg states that contribute high cross-section transitions to both the 1PA or 2PA spectrum can provide a reasonable description for the electronic structure of the bulk liquid. We believe that this justifies our approach in using a gas-phase electronic structure as a starting point to elucidate the nature of the transitions contributing to the condensed-phase electronic spectra.

VI. CONCLUSIONS

Broadband 2PA spectra for liquid methanol and ethanol have been presented for the first time. 2PA spectra are also simulated from first-principles for isolated methanol and ethanol molecules at the EOM-CCSD/d-aug-cc-PVDZ level of theory. The calculations form the basis for assigning the relatively featureless liquid-phase 2PA spectra but are particularly helpful in interpreting the polarization ratio. Relatively modest modifications of the computed in vacuo properties are necessary to reproduce the general features of the experimental spectra.

For both of the alcohols, the first excited state due to the 3s \leftarrow 2p_z transition is blue-shifted by 0.9 eV, as the upper Rydberg 3s orbital experiences Pauli repulsion due to the confinement by the solvent shell surrounding a single alcohol molecule.³⁴ Such a shift was known for water but was never confirmed for alcohols. As mentioned before, there was an apparent contradiction in the literature 61,72 concerning the gasto condensed-phase shift of the first electronic state in methanol. Our simulation of the 2PA spectra suggests that the 0.9 eV blue shift for the first transition in alcohols indeed mirrors the similar shift in water. Among all of the other transitions, those with an upper orbital having "s" character centered on the oxygen atom experience a similar blue shift of ~1 eV upon solvation. This is consistent with literature observations for the diatomic NO in solid matrices. 48,51 In contrast, our result indicates that an upper "s" orbital centered or spread onto carbon does not experience as large of a blue shift. This can be rationalized as follows: As the two oxygen lone pairs take part in hydrogen bonding, the promotion of an electron from the "out-of-plane" $O(2p_z)$ orbital to a primarily O(3s) Rydberg orbital (with a more spherical electron distribution) increases the electron density in the direction where the hydrogen bonding is present. Therefore, the upperstate electron wave function experiences a large Pauli repulsion that gives rise to such large blue shifts. Transitions involving the promotion of an electron into the "p"- or "d"-type diffuse Rydberg orbitals experience a smaller blue shift with correspondingly less Pauli repulsion and greater stabilization of their cationic core by the surrounding polar molecules. The higher-lying electronic states in ethanol experience relatively less destabilization, leading to less blue-shifted transitions (0.2 eV) as compared with methanol (0.33 eV). For the bigger alkyl substituent, the Rydberg state is more delocalized over the molecular framework, and the cation core is less screened for polarization stabilization by the surrounding dielectric.

Ab initio calculations show that the most intense peaks in the 2PA spectra correspond to the $3^{1}A_{1}$ transition in water and the $5A' \leftarrow 1A'$ transition in methanol and ethanol, and all of them are due to totally symmetric $2p_z-3p_z$ excitations. This means that substituting one of the hydrogens in water by a methyl or an ethyl group does not change the nature of the strongest transition dominating the 2PA spectra. Nevertheless, the calculated absolute 2PA cross-section for this transition drops from ~22 GM in MeOH to ~15 GM in EtOH. This is because the ethyl group has a larger effect on reducing the molecular symmetry, leading to a larger deviation of the 2pz-3p, transition from the "totally symmetric" regime; however, over the entire spectral region, the absolute 2PA cross section increases from methanol to ethanol. This points to the fact that an increasing number of electronic states contributes to the overall 2PA spectra, with larger alkyl groups thus compensating for the apparent decrease in the cross-section of the most intense transition.

We observe that the excitation-energy variation of the polarization ratio is similar for water and methanol. The decrease in the polarization ratio in the lower energy region results from an increasing contribution of the nontotally symmetric transitions (transitions to A" states; for example, $1A'' \leftarrow 1A'$). On the contrary, for ethanol (and longer alkyl substituents), the polarization ratio starts at ~ 3 in the lower energy region and shows less variation in the experimental window, maintaining a value >2.5 throughout. This suggests that transitions to the excited states of A" symmetry have relatively small cross sections in the 2PA spectra of higher alcohols, and the 2PA spectrum is dominated by totally symmetric transitions (transitions to A' states), even in the lower energy region. Such a difference in the polarization ratio helps us draw a very important conclusion. The electronic structure in higher alcohols, unlike methanol, is less dominated at lower energy by transitions involving oxygen-centered orbitals. The ethyl group blends in more carbon character to the lower and upper orbitals involved in the relevant electronic transitions and thus increasingly deviates from water.⁸⁷ This provides a good demonstration of the value of the polarization ratio in 2PA spectroscopy and how sensitive it is in capturing the character of electronic transitions in 2PA spectra.

Needless to say, the electronic structure of alcohols is much more complicated in the higher energy region, especially in the region approaching the ionization continuum. We can, however, use the gas-phase ab initio calculations and NTO analysis to speculate on the nature of the excitations across the recorded spectra. First, it is important to emphasize that the intense Rydberg transitions in the alcohol spectra fall well within our experimental spectral range, even after experiencing a general blue shift upon condensation to bulk. Removing these Rydberg transitions from the simulation, or drastically changing their cross-section from isolated-molecule calculations, results in a poor "fit" of the experimental spectra and the polarization ratio. This emphasizes the persistence of transitions in the condensed phase that resemble the properties of the Rydberg transitions in the gas phase. Our work shows that the Rydberg-like states seem to preserve their identity and the high cross-section of their transitions from the ground state in the liquid phase; this is a surprising result considering the large perturbations from the increasing number density, the polarization of the surrounding environment, and the near degeneracy of orbital energies across the neat liquid. In fact, the agreement between the experimental 2PA spectra and

simulations, which are based entirely on isolated-molecule calculations, indicates that the transitions can still be considered within a single molecule (atom-based) picture in the liquid phase possibly due to symmetry constraints rather than being better understood from a solid-state framework.

The broadband 2PA spectra presented here have provided a more complete picture of the electronically excited states for the simplest solvents that are heavily exploited for laser spectroscopy of dissolved solutes specifically because they lack π excitations. We have been able to comment on the 2PA band gap for these solvents, which is otherwise not possible through a single-color two-photon measurement. The 2PA threshold goes down to ~6.9 eV in methanol and ethanol as compared with that of water. Despite maintaining a very favorable effective band gap, we note that water has a 1 eV broader window that can be used for 2PA or UV pump-probe spectroscopy of dissolved solutes. We stress the importance of measuring the continuous polarization ratio spectrum, as it carries a valuable imprint of the individual transitions that matter the most in the 2PA spectra. Finally, perhaps surprisingly, isolated-molecule electronic structure calculations provide a very reasonable starting point to analyze the spectra. Realistic simulations are possible by shifting the energies of the calculated electronic states (with shift magnitudes consistent with past Rydberg spectroscopy in rare-gas matrices) and the selection of spectral broadening to match the experiment. This provides a semiquantitative picture of the solvatochromic shifts and spectral broadening required to describe the bulk spectroscopy of the neat solvent. Overall, we conclude by observing that a surprisingly large amount of information about the excited electronic transitions in important liquids can be extracted from apparently relatively featureless spectra.

ASSOCIATED CONTENT

S Supporting Information

The Supporting Information is available free of charge on the ACS Publications website at DOI: 10.1021/acs.jpca.9b04040.

1PA cross sections, 2PA cross sections, and polarization ratios of methanol and ethanol computed using 4.6 eV pump energy are tabulated. The 2PA spectra of propanol and butanol and their polarization ratios are also shown as a function of total excitation energy (PDF)

AUTHOR INFORMATION

Corresponding Author

 $\hbox{*E-mail: stephen.bradforth@usc.edu.}\\$

ORCID ®

Christopher G. Elles: 0000-0002-1408-8360 Stephen E. Bradforth: 0000-0002-6164-3347

Present Addresses

[†]Y.Z.: Department of Chemistry and Biochemistry, The Ohio State University, 100 West 18th Avenue, Columbus, OH 43210.

[‡]C.G.E.: Department of Chemistry, University of Kansas, 1567 Irving Hill Road, Lawrence, KS 66045.

Notes

The authors declare no competing financial interest.

■ ACKNOWLEDGMENTS

This work was supported by the National Science Foundation (experimental work under CHE-0617060 and theoretical work

under CHE-1665532). We thank Dr. Kaushik Nanda and Prof. Anna Krylov for helpful discussions regarding the calculation of two-photon properties. We also thank Sahil Gulania, Tirthendu Sen, and Dibyendu Mondal for help with application of the 2PA code in QChem. We acknowledge the Center for High Performance Computing at the University of Southern California for supercomputer time allocation.

REFERENCES

- (1) Bhawalkar, J. D.; He, G. S.; Park, C.-K.; Zhao, C. F.; Ruland, G.; Prasad, P. N. Efficient, Two-Photon Pumped Green Upconverted Cavity Lasing in a New Dye. *Opt. Commun.* **1996**, *124*, 33–37.
- (2) Brown, S. B.; Brown, E. A.; Walker, I. The Present and Future Role of Photodynamic Therapy in Cancer Treatment. *Lancet Oncol.* **2004**, *5*, 497–508.
- (3) Collins, H. A.; Khurana, M.; Moriyama, E. H.; Mariampillai, A.; Dahlstedt, E.; Balaz, M.; Kuimova, M. K.; Drobizhev, M.; Yang, V. X.; Phillips, D.; et al. Blood-Vessel Closure Using Photosensitizers Engineered for Two-Photon Excitation. *Nat. Photonics* **2008**, *2*, 420–424.
- (4) Ehrlich, J. E.; Wu, X. L.; Lee, I.-Y.; Hu, Z.-Y.; Röckel, H.; Marder, S. R.; Perry, J. W. Two-Photon Absorption and Broadband Optical Limiting with Bis-Donor Stilbenes. *Opt. Lett.* **1997**, *22*, 1843–1845.
- (5) He, G. S.; Bhawalkar, J. D.; Zhao, C. F.; Prasad, P. N. Optical Limiting Effect in a Two-photon Absorption Dye Doped Solid Matrix. *Appl. Phys. Lett.* **1995**, *67*, 2433–2435.
- (6) He, G. S.; Reinhardt, B. A.; Bhatt, J. C.; Dillard, A. G.; McKellar, R.; Xu, C.; Prasad, P. N. Two-Photon Absorption and Optical-Limiting Properties of Novel Organic Compounds: Erratum. *Opt. Lett.* **1995**, 20, 1930–1930.
- (7) Helmchen, F.; Denk, W. Deep Tissue Two-Photon Microscopy. *Nat. Methods* **2005**, *2*, 932–940.
- (8) Kawata, S.; Kawata, Y. Three-Dimensional Optical Data Storage Using Photochromic Materials. *Chem. Rev.* **2000**, *100*, 1777–1788.
- (9) LaFratta, C. N.; Fourkas, J. T.; Baldacchini, T.; Farrer, R. A. Multiphoton Fabrication. *Angew. Chem., Int. Ed.* **2007**, *46*, 6238–6258.
- (10) Parthenopoulos, D. A.; Rentzepis, P. M. Three-Dimensional Optical Storage Memory. *Science* **1989**, *245*, 843–845.
- (11) Spangler, C. Recent Development in the Design of Organic Materials for Optical Power Limiting. *J. Mater. Chem.* **1999**, *9*, 2013–2020
- (12) Walker, E.; Dvornikov, A.; Coblentz, K.; Rentzepis, P. Terabyte Recorded in Two-Photon 3D Disk. *Appl. Opt.* **2008**, *47*, 4133–4139.
- (13) Zhou, W.; Kuebler, S. M.; Braun, K. L.; Yu, T.; Cammack, J. K.; Ober, C. K.; Perry, J. W.; Marder, S. R. An Efficient Two-Photon-Generated Photoacid Applied to Positive-Tone 3D Microfabrication. *Science* **2002**, *296*, 1106–1109.
- (14) Reuther, A.; Laubereau, A.; Nikogosyan, D. N. A Simple Method for the in Situ Analysis of Femtosecond UV Pulses in the Pump-Probe Spectroscopy of Solutions. *Opt. Commun.* **1997**, *141*, 180–184.
- (15) Reuther, A.; Nikogosyan, D. N.; Laubereau, A. Primary Photochemical Processes in Thymine in Concentrated Aqueous Solution Studied by Femtosecond UV Spectroscopy. *J. Phys. Chem.* **1996**, *100*, 5570–5577.
- (16) Gong, S.-H.; Penzkofer, A. Two-Photon Absorption and Two-Photon-Induced Absorption of Some Organic Liquids at 347.15 Nm. *Opt. Quantum Electron.* **1999**, 31, 269–290.
- (17) Dragonmir, A.; McInerney, J. G.; Nikogosyan, D. N. Femtosecond Measurements of Two-Photon Absorption Coefficients at Λ = 264 Nm in Glasses, Crystals, and Liquids. *Appl. Opt.* **2002**, *41*, 4365–4376.
- (18) Dragornir, A.; McInerney, J. G.; Nikogosyan, D. N.; Ruth, A. A. Two-Photon Absorption Coefficients of Several Liquids at 264 Nm. *IEEE J. Quantum Electron.* **2002**, 38, 31–36.

- (19) Nikogosyan, D. N.; Oraevsky, A. A.; Rupasov, V. I. Two-Photon Ionization and Dissociation of Liquid Water by Powerful Laser UV Radiation. *Chem. Phys.* **1983**, *77*, 131–143.
- (20) Pommeret, S.; Gobert, F.; Mostafavi, M.; Lampre, I.; Mialocq, J.-C. Femtochemistry of the Hydrated Electron at Decimolar Concentration. *J. Phys. Chem. A* **2001**, *105*, 11400–11406.
- (21) Dragomir, A.; McInerney, J. G.; Nikogosyan, D. N.; Kazansky, P. G. Two-Photon Absorption Properties of Commercial Fused Silica and Germanosilicate Glass at 264 Nm. *Appl. Phys. Lett.* **2002**, *80*, 1114–1116.
- (22) Yamaguchi, S.; Tahara, T. Two-Photon Absorption Spectrum of All-Trans Retinal. *Chem. Phys. Lett.* **2003**, *376*, 237–243.
- (23) Yamaguchi, S.; Tahara, T. Observation of an Optically Forbidden State of C 60 by Nondegenerate Two-Photon Absorption Spectroscopy. *Chem. Phys. Lett.* **2004**, *390*, 136–139.
- (24) Drobizhev, M.; Karotki, A.; Kruk, M.; Rebane, A. Resonance Enhancement of Two-Photon Absorption in Porphyrins. *Chem. Phys. Lett.* **2002**, 355, 175–182.
- (25) Drobizhev, M.; Karotki, A.; Kruk, M.; Mamardashvili, N. Z.; Rebane, A. Drastic Enhancement of Two-Photon Absorption in Porphyrins Associated with Symmetrical Electron-Accepting Substitution. *Chem. Phys. Lett.* **2002**, *361*, 504–512.
- (26) Karotki, A.; Drobizhev, M.; Kruk, M.; Spangler, C.; Nickel, E.; Mamardashvili, N.; Rebane, A. Enhancement of Two-Photon Absorption in Tetrapyrrolic Compounds. J. Opt. Soc. Am. B 2003, 20, 321–332
- (27) Rebane, A.; Makarov, N. S.; Drobizhev, M.; Spangler, B.; Tarter, E. S.; Reeves, B. D.; Spangler, C. W.; Meng, F.; Suo, Z. Quantitative Prediction of Two-Photon Absorption Cross Section Based on Linear Spectroscopic Properties. *J. Phys. Chem. C* **2008**, *112*, 7997–8004.
- (28) Negres, R. A.; Hales, J. M.; Kobyakov, A.; Hagan, D. J.; Van Stryland, E. W. Two-Photon Spectroscopy and Analysis with a White-Light Continuum Probe. *Opt. Lett.* **2002**, *27*, 270–272.
- (29) Negres, R. A.; Hales, J. M.; Kobyakov, A.; Hagan, D. J.; Van Stryland, E. W. Experiment and Analysis of Two-Photon Absorption Spectroscopy Using a White-Light Continuum Probe. *IEEE J. Quantum Electron.* **2002**, *38*, 1205–1216.
- (30) De Wergifosse, M.; Houk, A. L.; Krylov, A. I.; Elles, C. G. Two-Photon Absorption Spectroscopy of Trans-Stilbene, Cis-Stilbene, and Phenanthrene: Theory and Experiment. *J. Chem. Phys.* **2017**, *146*, 144305.
- (31) de Wergifosse, M.; Elles, C. G.; Krylov, A. I. Two-Photon Absorption Spectroscopy of Stilbene and Phenanthrene: Excited-State Analysis and Comparison with Ethylene and Toluene. *J. Chem. Phys.* **2017**, *146*, 174102.
- (32) Houk, A. L.; Zheldakov, I. L.; Tommey, T. A.; Elles, C. G. Two-Photon Excitation of Trans-Stilbene: Spectroscopy and Dynamics of Electronically Excited States above S1. *J. Phys. Chem. B* **2015**, *119*, 9335–9344.
- (33) Houk, A. L.; Givens, R. S.; Elles, C. G. Two-Photon Activation of p-Hydroxyphenacyl Phototriggers: Toward Spatially Controlled Release of Diethyl Phosphate and ATP. *J. Phys. Chem. B* **2016**, *120*, 3178–3186.
- (34) Elles, C. G.; Rivera, C. A.; Zhang, Y.; Pieniazek, P. A.; Bradforth, S. E. Electronic Structure of Liquid Water from Polarization-Dependent Two-Photon Absorption Spectroscopy. *J. Chem. Phys.* **2009**, *130*, 084501.
- (35) Faubel, M.; Steiner, B.; Toennies, J. P. Photoelectron Spectroscopy of Liquid Water, Some Alcohols, and Pure Nonane in Free Micro Jets. *J. Chem. Phys.* **1997**, *106* (22), 9013–9031.
- (36) Bernas, A.; Grand, D. The So-Called Ionization Potential of Water and Associated Liquids. *J. Phys. Chem.* **1994**, *98*, 3440–3443.
- (37) Boyle, J. W.; Ghormley, J. A.; Hochanadel, C. J.; Riley, J. F. Production of Hydrated Electrons by Flash Photolysis of Liquid Water with Light in the First Continuum. *J. Phys. Chem.* **1969**, 73, 2886–2890.
- (38) Bartels, D. M.; Crowell, R. A. Photoionization Yield vs Energy in H2O and D2O. J. Phys. Chem. A 2000, 104, 3349-3355.

- (39) Elles, C. G.; Jailaubekov, A. E.; Crowell, R. A.; Bradforth, S. E. Excitation-Energy Dependence of the Mechanism for Two-Photon Ionization of Liquid H 2 O and D 2 O from 8.3 to 12.4 EV. *J. Chem. Phys.* **2006**, 125, 044515.
- (40) Reisler, H.; Krylov, A. I. Interacting Rydberg and Valence States in Radicals and Molecules: Experimental and Theoretical Studies. *Int. Rev. Phys. Chem.* **2009**, 28, 267–308.
- (41) Butler, L. J. Chemical Reaction Dynamics beyond the Born-Oppenheimer Approximation. *Annu. Rev. Phys. Chem.* **1998**, 49, 125–171.
- (42) Worth, G. A.; Cederbaum, L. S. Beyond Born-Oppenheimer: Molecular Dynamics through a Conical Intersection. *Annu. Rev. Phys. Chem.* **2004**, *55*, 127–158.
- (43) Stolow, A.; Bragg, A. E.; Neumark, D. M. Femtosecond Time-Resolved Photoelectron Spectroscopy. *Chem. Rev.* **2004**, *104*, 1719–1758
- (44) Stolow, A. Femtosecond Time-Resolved Photoelectron Spectroscopy of Polyatomic Molecules. *Annu. Rev. Phys. Chem.* **2003**, *54*, 89–119.
- (45) Stanton, J. F. Coupled-Cluster Theory, Pseudo-Jahn-Teller Effects and Conical Intersections. *J. Chem. Phys.* **2001**, *115*, 10382–10392
- (46) Russ, N. J.; Crawford, T. D.; Tschumper, G. S. Real versus Artifactual Symmetry-Breaking Effects in Hartree–Fock, Density-Functional, and Coupled-Cluster Methods. *J. Chem. Phys.* **2004**, *120*, 7298–7306.
- (47) Chergui, M.; Schwentner, N.; Tramer, A. Spectroscopy of the NO Molecule in N2 and Mixed N2/Kr Matrices. *Chem. Phys. Lett.* **1993**, 201, 187–193.
- (48) Vigliotti, F.; Chergui, M.; Dickgiesser, M.; Schwentner, N. Rydberg States in Quantum Crystals NO in Solid H 2. Faraday Discuss. 1997, 108, 139–159.
- (49) Chergui, M.; Schwentner, N.; Chandrasekharan, V. Rydberg Fluorescence of NO Trapped in Rare Gas Matrices. *J. Chem. Phys.* **1988**, *89*, 1277–1284.
- (50) Chergui, M.; Schwentner, N.; Böhmer, W. Rydberg States of NO Trapped in Rare Gas Matrices. *J. Chem. Phys.* **1986**, *85*, 2472–2482.
- (51) Vigliotti, F.; Chergui, M. Rydberg States in the Condensed Phase Studied by Fluorescence Depletion Spectroscopy. *Eur. Phys. J.* D **2000**, *10*, 379–390.
- (52) Vigliotti, F.; Zerza, G.; Chergui, M.; Rubayo-Soneira, J. Lifetime Lengthening of Molecular Rydberg States in the Condensed Phase. *J. Chem. Phys.* **1998**, *109*, 3508–3517.
- (53) Cheng, B.-M.; Bahou, M.; Chen, W.-C.; Yui, C.; Lee, Y.-P.; Lee, L. C. Experimental and Theoretical Studies on Vacuum Ultraviolet Absorption Cross Sections and Photodissociation of CH 3 OH, CH 3 OD, CD 3 OH, and CD 3 OD. *J. Chem. Phys.* **2002**, *117*, 1633–1640.
- (54) Philis, J. G. Resonance-Enhanced Multiphoton Ionization Spectra of Jet-Cooled Methanol and Ethanol. *Chem. Phys. Lett.* **2007**, 449, 291–295.
- (55) Scott, T. W.; Albrecht, A. C. A Rydberg Transition in Benzene in the Condensed Phase: Two-Photon Fluorescence Excitation Studies. *J. Chem. Phys.* **1981**, *74*, 3807–3812.
- (56) Whetten, R. L.; Grubb, S. G.; Otis, C. E.; Albrecht, A. C.; Grant, E. R. Higher Excited States of Benzene: Polarized Ultraviolet Two-Photon Absorption Spectroscopy. *J. Chem. Phys.* **1985**, 82, 1115–1134.
- (57) Mota, R.; Parafita, R.; Giuliani, A.; Hubin-Franskin, M.-J.; Lourenco, J. M. C.; Garcia, G.; Hoffmann, S. V.; Mason, N. J.; Ribeiro, P. A.; Raposo, M.; et al. Water VUV Electronic State Spectroscopy by Synchrotron Radiation. *Chem. Phys. Lett.* **2005**, *416*, 152–159.
- (58) Salahub, D. R.; Sandorfy, C. The Far-Ultraviolet Spectra of Some Simple Alcohols and Fluoroalcohols. *Chem. Phys. Lett.* **1971**, *8*, 71–74.
- (59) Heller, J. M., Jr; Hamm, R. N.; Birkhoff, R. D.; Painter, L. R. Collective Oscillation in Liquid Water. *J. Chem. Phys.* **1974**, *60*, 3483–3486.

- (60) Marin, T. W.; Janik, I.; Bartels, D. M.; Chipman, D. M. Vacuum Ultraviolet Spectroscopy of the Lowest-Lying Electronic State in Subcritical and Supercritical Water. *Nat. Commun.* **2017**, *8*, 15435.
- (61) Jung, J. M.; Gress, H. Single-Photon Absorption of Liquid Methanol and Ethanol in the Vacuum Ultraviolet. *Chem. Phys. Lett.* **2002**, 359, 153–157.
- (62) Link, O. Femtosekunden-Photoelektronenspektroskopie mit Extrem Ultravioletter Strahlung an Flüssigkeitsgrenzflächen. Ph.D. Thesis, Georg-August-Universität Göttingen, 2007
- (63) Robin, M. B. Higher Excited States of Polyatomic Molecules; Academic Press: New York, 1974; Vol. 1, p 180.
- (64) Katsumata, S.; Iwai, T.; Kimura, K. Photoelectron Spectra and Sum Rule Consideration. Higher Alkyl Amines and Alcohols. *Bull. Chem. Soc. Ipn.* **1973**, *46*, 3391–3395.
- (65) Baker, A. D.; Betteridge, D.; Kemp, N. R.; Kirby, R. E. Application of Photoelectron Spectrometry to Pesticide Analysis. II. Photoelectron Spectra of Hydroxy-, and Halo-Alkanes and Halohydrins. *Anal. Chem.* **1971**, *43*, 375–381.
- (66) Nee, J. B.; Suto, M.; Lee, L. C. Photoexcitation Processes of CH3OH: Rydberg States and Photofragment Fluorescence. *Chem. Phys.* **1985**, *98*, 147–155.
- (67) Robin, M. B.; Kuebler, N. A. Excited Electronic States of the Simple Alcohols. *J. Electron Spectrosc. Relat. Phenom.* **1972**, *1*, 13–28.
- (68) Tam, W.-C.; Brion, C. E. Electron Impact Spectra of Some Alkyl Derivatives of Water and Related Compounds. *J. Electron Spectrosc. Relat. Phenom.* **1974**, *3*, 263–279.
- (69) Feng, R.; Brion, C. E. Absolute Photoabsorption Cross-Sections (Oscillator Strengths) for Ethanol (5–200 EV). *Chem. Phys.* **2002**, 282, 419–427.
- (70) Hargreaves, L. R.; Khakoo, M. A.; Winstead, C.; McKoy, V. Excitation of the Lowest Electronic Transitions in Ethanol by Low-Energy Electrons. *J. Phys. B: At., Mol. Opt. Phys.* **2016**, 49, 185201.
- (71) Lucazeau, G.; Sandorfy, C. On the Far-Ultraviolet Spectra of Some Simple Aldehydes. *J. Mol. Spectrosc.* **1970**, *35*, 214–231.
- (72) Kuo, Y.-P.; Lu, H.-C.; Wu, Y.-J.; Cheng, B.-M.; Ogilvie, J. F. Absorption Spectra in the Vacuum Ultraviolet Region of Methanol in Condensed Phases. *Chem. Phys. Lett.* **2007**, 447, 168–174.
- (73) Tauber, M. J.; Mathies, R. A.; Chen, X.; Bradforth, S. E. Flowing Liquid Sample Jet for Resonance Raman and Ultrafast Optical Spectroscopy. *Rev. Sci. Instrum.* **2003**, *74*, 4958–4960.
- (74) Sander, M. U.; Luther, K.; Troe, J. Excitation Energy Dependence of the Photoionization of Liquid Water. *J. Phys. Chem.* **1993**, 97, 11489–11492.
- (75) Kovalenko, S. A.; Dobryakov, A. L.; Ruthmann, J.; Ernsting, N. P. Femtosecond Spectroscopy of Condensed Phases with Chirped Supercontinuum Probing. *Phys. Rev. A: At., Mol., Opt. Phys.* **1999**, 59, 2369.
- (76) Nanda, K. D.; Krylov, A. I. Two-Photon Absorption Cross Sections within Equation-of-Motion Coupled-Cluster Formalism Using Resolution-of-the-Identity and Cholesky Decomposition Representations: Theory, Implementation, and Benchmarks. *J. Chem. Phys.* **2015**, *142*, 064118.
- (77) Wirth, M. J.; Koskelo, A.; Sanders, M. J. Molecular Symmetry and Two-Photon Spectroscopy. *Appl. Spectrosc.* **1981**, *35*, 14–21.
- (78) Monson, P. R.; McClain, W. M. Polarization Dependence of the Two-Photon Absorption of Tumbling Molecules with Application to Liquid 1-Chloronaphthalene and Benzene. *J. Chem. Phys.* **1970**, *53*, 29–37.
- (79) Beerepoot, M. T.; Friese, D. H.; List, N. H.; Kongsted, J.; Ruud, K. Benchmarking Two-Photon Absorption Cross Sections: Performance of CC2 and CAM-B3LYP. *Phys. Chem. Chem. Phys.* **2015**, *17*, 19306–19314.
- (80) Krylov, A. I.; Sherrill, C. D.; Head-Gordon, M. Excited States Theory for Optimized Orbitals and Valence Optimized Orbitals Coupled-Cluster Doubles Models. *J. Chem. Phys.* **2000**, *113*, 6509–6527.
- (81) Stanton, J. F.; Bartlett, R. J. The Equation of Motion Coupledcluster Method. A Systematic Biorthogonal Approach to Molecular

- Excitation Energies, Transition Probabilities, and Excited State Properties. J. Chem. Phys. 1993, 98, 7029-7039.
- (82) Bartlett, R. J. The Coupled-Cluster Revolution. *Mol. Phys.* **2010**, *108*, 2905–2920.
- (83) Shao, Y.; Gan, Z.; Epifanovsky, E.; Gilbert, A. T.; Wormit, M.; Kussmann, J.; Lange, A. W.; Behn, A.; Deng, J.; Feng, X.; et al. Advances in Molecular Quantum Chemistry Contained in the Q-Chem 4 Program Package. *Mol. Phys.* **2015**, *113*, 184–215.
- (84) McClain, W. M. Excited State Symmetry Assignment Through Polarized Two-Photon Absorption Studies of Fluids. *J. Chem. Phys.* **1971**, *55*, 2789–2796.
- (85) Monson, P. R.; McClain, W. M. Complete Polarization Study of the Two-Photon Absorption of Liquid 1-Chloronaphthalene. *J. Chem. Phys.* **1972**, *56*, 4817–4825.
- (86) McClain, W. M. Two-Photon Molecular Spectroscopy. Acc. Chem. Res. 1974, 7, 129-135.
- (87) Zhang, Y. Two-Photon Absorption Spectroscopy and Excited State Photochemistry of Small Molecules. Ph.D. Thesis, University of Southern California, 2012.
- (88) Rasmusson, M.; Tarnovsky, A. N.; Åkesson, E.; Sundström, V. On the Use of Two-Photon Absorption for Determination of Femtosecond Pump—Probe Cross-Correlation Functions. *Chem. Phys. Lett.* **2001**, 335, 201–208.
- (89) Plasser, F.; Wormit, M.; Dreuw, A. New Tools for the Systematic Analysis and Visualization of Electronic Excitations. I. Formalism. *J. Chem. Phys.* **2014**, *141*, 024106.
- (90) Plasser, F.; Lischka, H. Analysis of Excitonic and Charge Transfer Interactions from Quantum Chemical Calculations. *J. Chem. Theory Comput.* **2012**, *8*, 2777–2789.
- (91) Plasser, F.; Bäppler, S. A.; Wormit, M.; Dreuw, A. New Tools for the Systematic Analysis and Visualization of Electronic Excitations. II. Applications. *J. Chem. Phys.* **2014**, *141*, 024107.
- (92) Tokushima, T.; Harada, Y.; Takahashi, O.; Senba, Y.; Ohashi, H.; Pettersson, L. G.; Nilsson, A.; Shin, S. High Resolution X-Ray Emission Spectroscopy of Liquid Water: The Observation of Two Structural Motifs. *Chem. Phys. Lett.* **2008**, *460*, 387–400.
- (93) Kashtanov, S.; Augustson, A.; Rubensson, J.-E.; Nordgren, J.; Ågren, H.; Guo, J.-H.; Luo, Y. Chemical and Electronic Structures of Liquid Methanol from X-Ray Emission Spectroscopy and Density Functional Theory. *Phys. Rev. B: Condens. Matter Mater. Phys.* **2005**, 71, 104205.
- (94) Larkins, F. P.; Seen, A. J. Ab Initio Studies of Molecular X-Ray Emission Processes: Methanol. *Phys. Scr.* **1990**, *41*, 827.
- (95) Wilson, K. R.; Cavalleri, M.; Rude, B. S.; Schaller, R. D.; Catalano, T.; Nilsson, A.; Saykally, R. J.; Pettersson, L. G. M. X-Ray Absorption Spectroscopy of Liquid Methanol Microjets: Bulk Electronic Structure and Hydrogen Bonding Network. *J. Phys. Chem. B* **2005**, *109*, 10194–10203.
- (96) Quickenden, T. I.; Irvin, J. A. The Ultraviolet Absorption Spectrum of Liquid Water. J. Chem. Phys. 1980, 72, 4416–4428.
- (97) Atlas, U. V. UV Atlas of Organic Compounds; Plenum Press: New York, 1966.
- (98) Pham, T. A.; Govoni, M.; Seidel, R.; Bradforth, S. E.; Schwegler, E.; Galli, G. Electronic Structure of Aqueous Solutions: Bridging the Gap between Theory and Experiments. *Sci. Adv.* **2017**, *3*, e1603210.
- (99) Pieniazek, P. A.; Sundstrom, E. J.; Bradforth, S. E.; Krylov, A. I. Degree of Initial Hole Localization/Delocalization in Ionized Water Clusters. *J. Phys. Chem. A* **2009**, *113*, 4423–4429.
- (100) Ghosh, D.; Roy, A.; Seidel, R.; Winter, B.; Bradforth, S.; Krylov, A. I. First-Principle Protocol for Calculating Ionization Energies and Redox Potentials of Solvated Molecules and Ions: Theory and Application to Aqueous Phenol and Phenolate. *J. Phys. Chem. B* **2012**, *116*, 7269–7280.
- (101) Ghosh, D.; Kosenkov, D.; Vanovschi, V.; Flick, J.; Kaliman, I.; Shao, Y.; Gilbert, A. T. B.; Krylov, A. I.; Slipchenko, L. V. Effective Fragment Potential Method in Q-CHEM: A Guide for Users and Developers. *J. Comput. Chem.* **2013**, *34*, 1060–1070.

- (102) Ghosh, D.; Isayev, O.; Slipchenko, L. V.; Krylov, A. I. Effect of Solvation on the Vertical Ionization Energy of Thymine: From Microhydration to Bulk. *J. Phys. Chem. A* **2011**, *115*, 6028–6038.
- (103) Gurunathan, P. K.; Acharya, A.; Ghosh, D.; Kosenkov, D.; Kaliman, I.; Shao, Y.; Krylov, A. I.; Slipchenko, L. V. Extension of the Effective Fragment Potential Method to Macromolecules. *J. Phys. Chem. B* **2016**, *120*, 6562–6574.
- (104) Chergui, M.; Schwentner, N. Experimental Evidence to Rydbergization of Antibonding Molecular Orbitals. *Chem. Phys. Lett.* **1994**, 219, 237–242.
- (105) Martí, J.; Padró, J. A.; Guàrdia, E. Hydrogen Bonding Influence on the Intermolecular Vibrational Spectra of Liquid Methanol. *J. Mol. Liq.* **1995**, *64*, 1–12.
- (106) Guàrdia, E.; Śesé, G.; Padró, J. A. On the Hydrogen Bonding Effects in Liquid Methanol: A Molecular Dynamics Simulation Study. *J. Mol. Liq.* **1994**, *62*, 1–16.
- (107) Saiz, L.; Padro, J. A.; Guardia, E. Structure and Dynamics of Liquid Ethanol. J. Phys. Chem. B 1997, 101, 78–86.
- (108) Portella-Oberli, M. T.; Jeannin, C.; Chergui, M. Ultrafast Dynamics of Rydberg States in the Condensed Phase. *Chem. Phys. Lett.* **1996**, 259, 475–481.
- (109) Morikawa, E.; Köhler, A. M.; Reininger, R.; Saile, V.; Laporte, P. Medium Effects on Valence and Low-n Rydberg States: NO in Argon and Krypton. *J. Chem. Phys.* **1988**, *89*, 2729–2737.